

Motions in waves

8.1 Introduction

The purpose of this chapter is to introduce the reader to ACV and SES vehicle dynamics. In a seaway (or over rough terrain for amphibious ACVs), the craft will respond to the undulating surface by pitching, heaving and rolling as it moves forward along its track. Dynamic sway and yaw motions may also be significant for ACVs over undulating terrain. These motions are generally considered together with design of the craft control systems, rather than as analysis of the motions themselves, (see Chapter 7). We will concentrate in this chapter on the heave, roll and pitch, which govern ride quality and speed loss in a seaway.

The cushion system responds as a damped spring system, while movement of the skirt and SES sidehulls into and out of the water induce varying lift and drag forces. The forces do not vary linearly. Initial models for ACV and SES motion attempted to linearize the response, to make prediction simpler. More recently, nonlinear solutions have been proposed and are now being further developed. We present these theories later in this chapter, after reviewing the main parameters which affect ACV and SES motions.

The objectives in carrying out such analyses are to identify the motion characteristics themselves as an input into defining:

- instability boundaries, e.g. plough-in, heave bounce and cobblestoning;
- criteria for dynamic stability, to compare with static stability requirements from Chapter 2;
- passenger and operating personnel motion response and so assessment of ride quality;
- assessment of externally excited vibration.

Hovercraft seaworthiness

An ACV is able to display the special characteristics for which it is best known while running at high speed over shallow water, rapids, ice and swamp – places no other craft can go. While these ‘special abilities’ interest many military and civil users with particular mission requirements, such environments do not include the wind-driven waves found in an open seaway. Generally, a craft’s capabilities in an open seaway will

control its transit capabilities between locations where a special mission may be required.

Meanwhile, the SES can best demonstrate its own high speed and work capacity relative to displacement vessels in light weather conditions in a seaway. Where the environmental conditions are favourable, the SES is capable of demonstrating significantly higher transport efficiency than other vehicles.

In conditions typical of an open seaway, the seaworthiness of current ACV/SES still leaves a lot to be desired, especially in comparison with deep submerged hydrofoil craft, or larger high speed catamaran ferries. Part of the problem is that an ACV or SES has a higher work capacity than the competing craft, so that the comparison is almost always with a larger vessel. In a seaway, once vessel length is significantly less than L_s , the mean length of waves of height H_s , it will follow the wave surface profile, with much increased motions. A smaller ACV or SES travelling at higher speed than a more conventional vessel therefore needs a cushion system which can reduce motions by being 'responsive'.

Other key points distinguishing ACV and SES response from conventional vessels are as follows:

1. Amphibious hovercraft hydrodynamic drag is very small in calm conditions. In the case where the craft runs in waves, there will be a rapid build-up of skirt drag and speed degradation, unless the skirt and cushion system is very responsive to the waves. Such skirt systems are only now reaching the point where safe craft can be designed for high-speed operation.
2. While there is a small area in contact with the water surface on an ACV, it has a large frontal area (mostly the skirt area actually), leading to a large air profile drag when running into head winds, in a similar way to the build-up of hydrodynamic resistance of a conventional ship running in head seas. Moreover, the air propeller thrust will be reduced, leading to additional speed degradation. Further, the manœuvrability also deteriorates as described in Chapter 6.

Ducted propulsors can be designed to have lower thrust degradation, while remaining as quiet as a large open propeller and so minimize these problems. SES powered by water jets or high speed propellers have the same design problem as any high-speed ship (see Chapter 15).

3. Wave pumping, motion pumping and the rapid changes of skirt air leakage area of hovercraft running in waves all lead to significant vertical acceleration. This can affect the operation of machinery, engines, equipment and crews etc. Use of a responsive skirt system and/or a cushion air damping system ('ride control system') can improve this enormously. This technology has been developed during the 1980s and needs further work to give really smooth ride quality at high speed.

Developments over the last decade have improved responses through the low-pressure amphibious ACV skirt and SES cushion venting systems. The design basis is now available; it is a matter of extending application to larger vessels.

Historical review

While the performance of early ACVs on calm water was very impressive, this was not the case in rough seas. Hovercraft dynamic motions were uncomfortable due to high

vertical accelerations. Speed loss and reduced manœuvrability in a seaway of some early craft were significant, resulting in a marginal ability to stay above hump speed.

Much research effort has therefore been applied to find ways to improve the seaworthiness of ACV/SES, with the aim to reduce craft motions and accelerations and allow higher speeds in a given sea state, in order to improve transport efficiency.

Initial work was concentrated on improving stability. Once ACV designers had found ways to provide acceptable dynamic stability with low-pressure ratio skirts, their attention turned to improving ride quality by improving its responsiveness to waves. SES designers initially experimented with sidewall displacement ratio and geometry, also in the search for optimum balance between dynamic stability and drag, before turning to ride quality, in this case by use of cushion air venting systems.

In the 1960s Sir Christopher Cockerell in the UK together with the research staff at Hovercraft Development Ltd studied the motion of hovercraft in waves, considering the wave effects on the cushion as a piston moving in a cylinder as an adiabatic process. This showed hovercraft motions to generate high vertical acceleration. Benya [9] considered hovercraft as a rigid body, similar to conventional ships and derived differential equations of motion with multiple degrees of freedom from an analytical basis. Unfortunately, he did not make clear how to determine the various derivatives (static force and rotary moment derivatives) in his differential equations, and their physical meaning.

In the late 1960s Beardsley [16] began introducing the wave pumping concept for hovercraft running in waves and predicted that the wave pumping motion would strongly affect the seaworthiness and vertical acceleration of hovercraft. He maintained that a hovercraft had to be designed with enough reserve lift power to reduce the vertical acceleration of hovercraft in the case where craft were travelling in waves. At that time, most researchers were interested in the static hovering theory of hovercraft and so they did not realize the significance of Beardsley's work.

In 1972 Reynolds of the UK [67] first derived the linear equations of motion for hovercraft based on the condition that skirts do not physically come into contact with the water surface. The Froude–Krilov hypothesis was assumed to be valid and he did not consider the response of an air duct–fan–skirt system to waves. Reynolds then derived the coupled heaving equations of motion for an ACV and obtained a mathematical solution of the equations.

In the 1970s, Doctors [68], and Zhou, Yun and Hua [69, 70], developed nonlinear equations of motion for hovercraft and obtained a numerical solution by iteration. Although the equations and their numerical solution were more complicated, solution by time-step iteration for several wave frequencies of a hovercraft in regular waves could be obtained with the aid of a computer. The solution gave the researchers insight into the full process of craft motions in waves. In the equations, not only the nonlinear system of fan–air duct–skirt, but also the compressibility of cushion pressure of hovercraft moving in waves was introduced.

Lavis of the USA first pointed out the effect of compressibility of cushion air on the seaworthiness of hovercraft moving in waves and predicted that great distortion would occur to the prediction of seaworthiness quality of craft from model experiments in a towing tank [71], caused by air cushion compressibility not being able to be scaled correctly. However, researchers and designers were still interested in experimental investigations using scale model tests and real ship trials to determine

seaworthiness of ACV/SES. References 72–76 give details of such work for example. Such tests demonstrated that the scale model test results could be considered as valuable data as long as the model (ship) speed was not too high and the encounter frequency causing pitching/rolling of the craft was not too large.

Moran [73] considered that the cushion pressure of an SES with high L_c/B_c at high speed was not uniformly distributed, but had a spatially non-uniform distribution. He expected the motion equations of seaworthiness mentioned above would therefore be altered.

Even though the experts have different points of view on the theoretical investigation of hovercraft motion in waves, in general they have considered that if the scale ratio of a model is not too great and the craft speed as well as the encounter frequency of craft (model) are not too high, then the predictions based either on experimental results of scale models or solution of nonlinear differential equations of motion can give accurate results. This theory is based upon the following assumptions:

- Froude–Krilov hypothesis applies (similar to conventional ships).
- Cushion pressure is uniformly distributed.
- The flexible skirt is considered as the rigid body, namely the skirt fingers will be deformed when the skirt encounters waves, but considering the skirt as a body, the skirt bag is not responsive to the waves.

This theory only considers the fan/air duct/air cushion/hull integrated motion system and does not consider the motion response of a skirt with one or two degrees of freedom. Such assumptions may be reasonable in the case of a skirt with small response, but will lead to significant errors in the case of a modern responsive flexible skirt. In this chapter we will introduce calculation methods for ACV and SES motions in waves, as follows:

- transverse motions of an SES in beam seas (coupled roll and heave motion);
- longitudinal motion of an SES in head seas (coupled pitch and heave motion);
- longitudinal motion of an ACV in waves using the linear equations of motion.

All of these are considered as coupled motions with three degrees of freedom (i.e. roll, pitch and heave together with cushion pressure).

Linear equations of motion and the solution methods using the nonlinear equations of motion are both discussed in this chapter during the investigation of longitudinal motions of ACV/SES.

After considering the basic equations of motion, we will also review some key design issues for ACV/SES running in short-crested waves:

- the ‘cobblestone’ effect
- SES plough-in motion in following waves
- ACV speed degradation in head winds

and discuss the effect of various factors on seaworthiness of ACV/SES.

Characteristic features of ACV and SES motions in waves

Since hovercraft are supported by an air cushion, a number of motion features are characteristic to ACV/SES running in waves. The Froude–Krilov hypothesis, coupled

vibration of skirt/air duct/fan, nonlinear effects of fans and skirts, effect of cushion air compression, spatial distribution of cushion pressure, determination of cushion damping and added mass all constitute a series of challenges in the investigation of ACV and SES seaworthiness in waves. The questions raised by each of these issues may be summarized as follows.

Rigid body dynamics

The ACV is a rigid body, just the same as a conventional ship, so coupled motions with six degrees of freedom occur to ACV/SES running in waves. Meanwhile the craft are supported by an air cushion, so motions within the six degrees of freedom are strongly influenced by cushion pressure variations, hydrodynamic forces acting on skirts and aerodynamic characteristics of fans, air ducts and the cushion chamber. The hovercraft can thus be considered as a more complicated vibration system with multiple degrees of freedom, i.e. fan/air ducts/skirt/air cushion/hull, as additional parameters to the motions.

Froude–Krilov hypothesis

The Froude–Krilov hypothesis that the passing wave shape is not affected by the hull of the vessel is an important hypothesis to be considered in studying ship motions in waves. By this assumption, any reflected or radiated wave energy is ignored. But does an air cushion affect the shape of waves while the same wave is passing through a hovercraft cushion?

Since there is a difference in density of 800 to 1 between the water in the waves and the pressurized air cushion, such an effect may be considered small. The skirt of an amphibious ACV is more likely to act as a damper rather than as a source of radiated wave energy. The hulls of an SES will be subject to the same inaccuracy as for a displacement ship, with the additional complication of the interaction of catamaran hulls.

Model tests of hovercraft have not so far provided clear data to identify deviations from the Froude–Krilov hypothesis. At present then, the Froude–Krilov hypothesis is used without any special correction factors, to determine the basic motion response of a hovercraft to waves.

Cushion pressure fluctuations

Cushion pressure will fluctuate rapidly while hovercraft are running in waves, which leads to the lift fan(s) operating off the design point and possibly causing nonlinear effects of the fan characteristics. In addition, the high-frequency fluctuation of cushion pressure causes a dynamic response with a hysteresis effect of the fans. These factors lead to considerable complications in the study of hovercraft seaworthiness.

Skirt contact drag

While hovercraft are running in waves, sometimes the skirts' contact with the water surface will cause skirt response and hydrodynamic effects on the skirts. Sometimes the skirt will leave the water surface causing an additional area of air leakage. For this reason, the nonlinear effects of skirts on craft motion will be strong. In general, because the air gap under the skirts is very small, the craft skirt will come into contact with the water surface when rolling or pitching. In addition, the skirt contact will

lead to the hydrodynamic interaction which will induce skirt fluctuation and affect the pressure of the air cushion and craft motion.

Wave pumping

Forward motion of the air cushion in waves will create wave pumping as described in Chapter 2 and will also cause compression of the air cushion similar to the motion of an engine piston in its cylinder (in the case where the peripheral skirts are sealed). Thus, on what basis does it progress in the cushion? An adiabatic process (constant temperature), or some other process? At present the process is assumed adiabatic.

Spatial distribution of cushion pressure

In the case where ACV/SES are rolling in waves at high speed and high frequency, is it possible to assume that the cushion pressure is uniformly distributed, or specially distributed non-uniformly? If the latter, what effect would this have on craft response? So far there are no analytical methods to predict this response.

Determination of damping coefficient and coefficient of added mass

While hovercraft are pitching, rolling and heaving in waves, sometimes craft are suspended in the air, sometimes they are in the water, thus added mass and damping coefficients clearly vary with time. Accurate determination of the damping coefficient due to wave-making is therefore difficult and simplifying assumptions have to be made.

Key craft parameters

Before we develop equations of motion for SES and ACVs it is useful to identify some of the key parameters which may be used to evaluate a design. In Chapter 4, SES and ACV stability was analysed. From this analysis we should be able to derive the following parameters.

- heave stiffness
- heave natural period
- cushion resonance frequencies
- pitch stiffness
- pitch natural period
- roll stiffness
- roll natural period
- damping in heave, pitch and roll

With these data, considering each motion in turn and the SES or ACV as a simple spring and dashpot system it is possible using the natural period and damping coefficient to assess the response to any wave frequency.

If the natural period in pitch or roll is close to the period of maximum energy for the sea spectrum T_p and so is likely to give high responses in the operational sea state, then it will be worth while altering the cushion system to change the natural period.

It is useful to keep in mind the craft characteristics when reviewing the results of motions analysis as presented below.

8.2 Transverse motions of SES in beam seas (coupled roll and heave) [77]

In this section, we will discuss the transverse motion of an SES in beam seas. The transverse motion of an ACV can be dealt with by similar methods.

In Chapter 4 we introduced the calculation for transverse stability of an SES hovering statically, running in calm water. The transverse stability of an SES operating on inland waterways can be estimated using these methods as the surface will be relatively calm.

In the case where an SES travels in a river estuary, coastal area or open seaway, the combined action of winds and waves on the transverse stability and safety of the SES also has to be included. This is to establish appropriate stability criteria to determine the safety margin against overturning of a seagoing SES.

When an SES travels hull-borne (floating rather than hovering), the calculation of SES roll motion can be dealt with in the same way as the calculation of that for conventional displacement for planing craft such as catamarans [78, 79]. In the case where SESs are cushion borne in waves, the rolling motions of an SES will be rather different from that in the off-cushion condition.

As an example, the Chinese SES model 717C had a satisfactory operating speed, but on cushion, particularly in the planing condition above hump speed under the action of beam waves, it rolled slowly with a large amplitude. Due to the wide craft beam, the cushion air would leak under one sidewall in the case of slight roll angle, which enlarged the roll angle and caused a sense of instability to passengers, making them uneasy.

It is important therefore to study the transverse motion of SES in beam seas, particularly in the case of high cushion length-beam ratio. In order to easily compare the calculation with the experimental results, we temporarily do not consider the effect of craft speed and swaying motion and only investigate the coupled roll and heave motion of SES in beam seas.

Basic assumptions

1. We neglect the effect of sidewall and skirt immersion on the local wave profile, but the effect of cushion pressure on waves is taken into account, i.e. the Froude–Krilov hypothesis is used.
2. Uniform distribution of cushion pressure is assumed and the cushion plane is simplified as a rectangle.
3. The change of air density and pressure inside the air cushion are considered adiabatic, but the air flow of cushion air into the atmosphere is considered incompressible.
4. Fan revolutions are kept constant and the effect of fan dynamic response is neglected.
5. Added mass and damping force of a single sidewall can be estimated from test results for conventional craft and the cross-section of a sidewall is taken as a trapezoid to simplify the calculation.
6. The wave-damping force caused by the air cushion is neglected.

Coordinate system and nomenclature

Two right-hand coordinate systems are used in the equations. The coordinate system $GXYZ$ is the body coordinate system, with its origin point taken to go through the craft CG. In the global fixed coordinate system $O\xi\eta\zeta$, the undisturbed water surface is taken to be the base plane and the origin point is taken as point 0. We also assume that the GZ axis goes through the point 0 (as shown in Fig. 8.1) during the motion of the craft. The following parameters are defined:

Z_{sw}	Vertical distance from the CG to the base-line of the sidewalls (m)
H_b	" " wet deck (m)
Z_s	" " lower edge of the bow/stern seals (m)
Z_{Hl}	Average distance between the base-line and outer hard chine of sidewalls (m)
B_s	Max. thickness of the sidewalls (m)
B_B	Width of keel plate at various stations (m)
β_{1i}	Outer deadrise angle of the sidewall at various stations, ($^{\circ}$)
β_{2i}	Inner deadrise angle of the sidewall at various stations ($^{\circ}$)
P_c	Cushion pressure (N/m^2)
ζ_A	Wave amplitude (m)
L_w	Wavelength (m)
ω	Circular frequency of waves (Hz)
ζ_w	Vertical position of wave surface with respect to sea level (m)
L_c	Cushion length (m)
B_c	Cushion width at base plane of craft (m)
Q_i	Total flow rate of fans (m^3/s)
Q_e	Total air leakage flow rate under bow/stern seal (m^3/s)
Q_v	Flow rate due to the cushion compressibility (m^3/s)
Q_w	Flow rate due to the volume change rate of air cushion in wave (m^3/s)
$V_{is,B}$	Leakage velocity of cushion air under the seals and sidewall (m/s)
$\rho_{w,a}$	Density of the water and air (Ns^2/m^4)
$\gamma_{w,a}$	Specific weight of water and air (N/m^3)
$N_{R,L(i)}$	Heaving damping coefficient per unit length of the right/left sidewalls at various stations
$\lambda_{R,L(i)}$	Added mass coefficient per unit length of the right/left sidewalls at various stations
I_θ	Roll moment inertia of craft (Ns^2/m^3)
W	Weight of craft (N)

Suffixes R and L represent right and left.

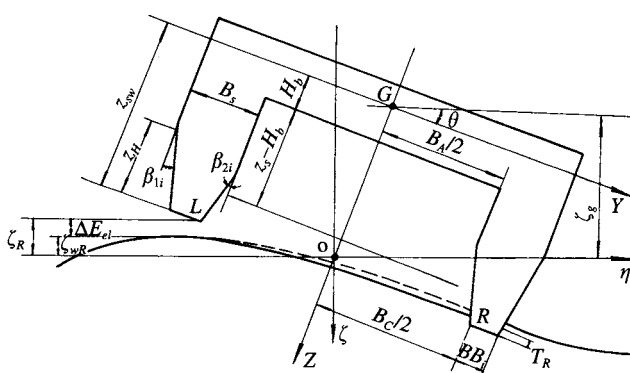


Fig. 8.1 Principal parameters of SES when rolling.

The nonlinear differential equations of motion

Calculation of draft and air leakage under sidewalls (Fig. 8.1)

The top width of air cushion chamber can be written as

$$B_A = 2Z_H \tan \beta_0 + 2BB_0 + B_c - 2B_s$$

where Z_H is the average vertical distance between the base-line and outer chine of the sidewall, β_0 the deadrise angle of sidewalls at mid-section of craft, BB_0 the width of keel plate at mid-section of craft, B_c the cushion beam at base plane of craft and B_s the thickness of the sidewalls.

If we assume the craft roll angle in waves is θ (starboard down positive), then the coordinates of points R and L located at sidewall base plane in the $0\xi\eta\zeta$ co-ordinate system are as in Fig. 8.1.

$$\eta_R = \eta_g + 0.5B_c \cos \theta - Z_{sw} \sin \theta \quad (8.1)$$

$$\zeta_R = \zeta_g + 0.5B_c \sin \theta + Z_{sw} \cos \theta$$

$$\eta_L = \eta_g - 0.5B_c \cos \theta - Z_{sw} \sin \theta \quad (8.2)$$

$$\zeta_L = \zeta_g - 0.5B_c \sin \theta + Z_{sw} \cos \theta$$

where Z_{sw} is the vertical distance between the CG of the craft and base-line of sidewalls (m).

The characteristic equation of beam waves in absolute coordinates is

$$\zeta_w = \zeta_A \cos (2\pi/L_w \eta - \omega t) \quad (8.3)$$

where ζ_A is the wave amplitude (m), ω the circular frequency of the wave (Hz), t the time (s) and L_w the wavelength (m).

In the GXYZ coordinate system, one takes $\eta = y \cos \theta$, then

$$\zeta_w = \zeta_A \cos [(2\pi/L_w) y \cos \theta - \omega t] \quad (8.4)$$

The wave elevations at points R and L are then

$$\zeta_{wR,L} = \zeta_A \cos (\pi B_c / L_w \cos \theta - / + \omega t) \quad (8.5)$$

The air leakage gaps at each sidewall are

$$\Delta Z_{eR,L} = \zeta_{wR,L} + p_e / \gamma_w - \zeta_{R,L} \quad (8.6)$$

The air leaks from the air cushion under the sidewalls when $\Delta Z_{eR,L} > 0$. When $\Delta Z_{eR,L} < 0$, the sidewall immerses in the water and the draft of sidewalls is

$$\begin{aligned} T_{R,L} &= -\Delta Z_{eR,L} \\ &= -\zeta_A \cos (\pi B_c / L_w \cos \theta - / + \omega t) - p_e / \gamma_w + \zeta_g \pm 0.5B_c \sin \theta + Z_{sw} \cos \theta \end{aligned} \quad (8.7)$$

where ζ_g is the height of the CG of the craft in the $0\xi\eta\zeta$ coordinate system.

The vertical velocity and acceleration of $T_{R,L}$ can be expressed by

$$\begin{aligned} \dot{T}_{R,L} &= -/ + \zeta_A \sin \theta (\pi B_c / l_c \cos - / + \omega t) - \dot{p}_c / \gamma_w \\ &\quad + \dot{\zeta}_g \pm 0.5B_c \cos \theta \dot{\theta} - Z_{sw} \sin \theta \dot{\theta} \end{aligned} \quad (8.8)$$

$$\ddot{T}_{R,L} = \zeta_A \omega^2 \cos(\pi B_c/l_c \cos \theta - / + \omega t) - \ddot{p}_c/\gamma_w + \ddot{\xi}_g \pm 0.5 B_c \cos \theta \ddot{\theta} - Z_{sw} \cos \theta \ddot{\theta} \quad (8.9)$$

where the second-order terms are neglected.

With regard to the difference in draft of sidewalls, p_c/γ_w , between outer and inner sides, the sidewall draft for buoyancy calculation can be expressed as follows, to simplify the calculation:

$$T_{R,L1} = T_{R,L} + p_c/\gamma_w \quad (8.10)$$

However, when one calculates the added mass and heave damping force of a sidewall, the sidewall draft can be written as

$$T_{R,L1} = T_{R,L} + p_c/(2\gamma_w) \quad (8.11)$$

Air cushion and lift fan system

1. Continuity equation of flow

$$Q_i = Q_e + Q_w + Q_v \quad (8.12)$$

$$Q_e = Q_{esw} + Q_{es} = Q_{eswR} + Q_{eswL} + Q_{es} \quad (8.13)$$

where Q_i is the total flow rate of the fan (m/s), Q_e the total air leakage flow rate under the bow/stern seals and sidewalls (m/s), Q_w the flow rate due to the volume change rate of air cushion in waves (m/s), Q_v the flow rate due to the cushion compressibility (m^3/s), Q_{esw} the flow rate under the sidewalls (m^3/s), and Q_{es} the flow rate under the bow/stern seals (m^3/s).

Assume the air leakage rate under the sidewall is A_{esw} , then the area of air leakage under the sidewalls is

$$A_{esw} = A_{eswR} + A_{eswL}$$

$$A_{eswR,L} = 0.5 L_c (\Delta Z_{eR,L} + |\Delta Z_{eR,L}|) \quad (8.14)$$

Then the flow under the sidewalls can be written as

$$Q_{eswR,L} = V_{ib} A_{eswR,L} \phi$$

where V_{ib} is the velocity of air leakage, which can be written as

$$V_{ib} = (2p_c/\rho_a)^{0.5} \operatorname{sgn}(p_c) \approx 4 \cdot (|p_c|)^{0.5} \operatorname{sgn}(p_c) \quad (8.15)$$

and ϕ is the flow rate coefficient, normally $\phi = 0.6 - 0.7$.

Considering the craft trim angle to be very small, the air leakage gap under the bow/stern seals can be written as follows (see Fig. 8.1)

$$\Delta Z_{es} = (p_c/\gamma_w) \sec \theta + \zeta_A \cos[(2\pi/L_w)y \cos \theta - \omega t] \sec \theta - \zeta_g \sec \theta - y \tan \theta - z_s \quad (8.16)$$

where z_s is the distance between the vertical CG and lower tip of bow/stern seals (m), and y the abscissa of the section at which the gaps of air leakage under the bow/stern seal are calculated. Thus the air leakage area A_{es} can be written as

$$A_{es} = \int_{-B_c/2}^{B_c/2} (\Delta Z_{es} + |\Delta Z_{es}|) dy \quad (8.17)$$

The velocity of air leakage under the bow and stern seals can be written

$$V_{is} = 4(|p_c|)^{0.5} \operatorname{sgn}(p_c)$$

Therefore

$$Q_{es} = A_{es} V_{is} \phi \quad (8.18)$$

We assume the change of air density in the cushion depends upon the law of adiabatic change, and the air density in the cushion at the static hovering condition is equal to that in the atmosphere, i.e.

$$p/(\rho_a v) = \text{constant}$$

where p is the total pressure in the air cushion, $p = p_c + p_a$, p_a the atmospheric pressure and v the adiabatic coefficient. In general $v = 1.4$. Thus the expression can be written as

$$\dot{\rho}_a/\rho_a = \dot{\rho}_a/(v(p_c + p_a))$$

Therefore

$$Q_w + Q_v = \frac{1}{\rho_a} \frac{d}{dt} (\rho_a V_c) = \dot{V}_c + V_c \frac{\dot{p}_c}{(1.4(p_a + p_c))} \quad (8.19)$$

where V_c is the volume of air cushion (m^3).

Assume $Z_v(y)$ represents the distance between the wave surface and the wet deck of the craft, then

$$\begin{aligned} Z_v(y) &= \zeta_w \sec \theta + p_c/\gamma_w \sec \theta - \zeta_g \sec \theta - y \tan \theta - H_b \\ V_c &= K_v l_c \int_{-B_c/2}^{B_c/2} Z_v(y) dy \\ &= K_v S_c [p_c/\gamma_w \sec \theta - H_b - \zeta_g \sec \theta \\ &\quad + [\zeta_A/(\pi B_c/L_w)] \sec^2 \theta \sin[(\pi B_c/L_w) \cos \theta] \cos \omega t] \end{aligned} \quad (8.20)$$

where S_c is the cushion area (m^2), $S_c = l_c B_c$ and K_v the correction coefficient for simplified sidewall configuration which leads to a calculation error on cushion volume. In general, we take $K_v = 0.90-1.1$. Therefore

$$\begin{aligned} \dot{V}_c &= K_v S_c [\dot{p}_c/\gamma_w \sec \theta - H_b - \dot{\zeta}_g \sec \theta \\ &\quad - [\zeta_A \omega L_w/(\pi B_c)] \sec^2 \theta \sin[(\pi B_c/L_w) \cos \theta] \sin \omega t] \end{aligned} \quad (8.21)$$

2. Pressure head equation

$$H_j = p_c + 0.5 \rho_a \xi (q_i/S_i)^2 \quad (8.22)$$

where H_j is the fan total pressure head (N/m^2), S_i the hole area for air inflow into the air cushion (m^2) and ξ the air duct head loss coefficient due to air blown from the fan outlet directly into the cushion (actually the calculation will be carried out using the head loss coefficient of the air ducts).

3. Fan characteristic equation

We will assume that there are two fans located on the craft, thus the inflow rate for each fan is equal to $Q_i/2$, so the equation for fan characteristics can be written as

$$H_j = A + BQ_i/2 - CQ_i^2/4 \quad (8.23)$$

where A, B and C are the dimensional coefficients of the fan characteristic and can be written as

$$A = A_{f0}\rho_a \cdot \pi^2 D_f^2 \eta_f^2 / 3600$$

$$B = B_{f0}\rho_a \eta_f / (15D_f)$$

$$C = C_{f0} 16\rho_a / (\pi^4 D_f^4)$$

where A_{f0} , B_{f0} , C_{f0} are the non-dimensional coefficients of fan characteristics, D_f the fan diameter (m) and η_f the revolution of the fan (r/min).

Cushion force (moment)

1. Cushion force F_c

Assume a_w , which represents the wave steepness across the craft width, can be defined as follows:

$$a_w = (\zeta_{wR} - \zeta_{wL})/B_c$$

The cushion force F'_c perpendicular to the average wave surface can be written as

$$F'_c = p_c S_c \sec(\theta - a_w)$$

Thus F_c , the projection of F'_c on the ζ axis, can be expressed by

$$F_c = -F'_c \cos a_w \quad (8.24)$$

2. Cushion moment M_c

Assume that cushion force F'_c acts on the origin point 0 of the coordinate system $0\xi\zeta$, then M_c represents the cushion moment about the CG of the craft and can be written by

$$M_c = -F'_c L F'_c = -p_c S_c \zeta_g \tan(\theta - a_w) \quad (8.25)$$

Force (moment) acting on skirts F_s

The force (moment) acting on the skirts can be expressed by

$$F_s = -p_c/2 (\cot a_1 + \cot a_2) \int_{-B_s/2}^{B_s/2} (-\Delta Z_{es} + |\Delta Z_{es}|) dy \quad (8.26a)$$

$$M_s = -p_c/2 (\cot a_1 + \cot a_2) \int_{-B_s/2}^{B_s/2} (-\Delta Z_{es} + |\Delta Z_{es}|) y dy \quad (8.26b)$$

where F_s is the hydrodynamic force on the skirts (N), M_s the hydrodynamic moments on skirts (Nm) and a_1 , a_2 the inclination angle of bow/stern seals with respect to axis GX(°).

Forces and moments acting on sidewalls (Fig. 8.2)

If $S_{R,L(i)}$ represents the immersion cross-section area of sidewalls at station i , then it can be written as

$$S_{R,L(i)} = 1/8 (\tan \beta_{1i} + \tan \beta_{2i})(T_{R,L1} + |T_{R,L1}|)^2 + 0.5BB_i(T_{R,L1} + |T_{R,L1}|) \quad (8.27)$$

where β_{1i} , β_{2i} are the outer and inner deadrise angles of the sidewall at station i ($^{\circ}$) and BB_i the width of the base-line at station i (m).

There are three cases to be considered with respect to the hydrodynamic forces acting on the craft during craft motion according to the different draft of port and starboard sidewalls; they are described as follows.

Case 1: Cushion air leaks under the port sidewall, but starboard is immersed

$$\begin{aligned} F_{swR} &= \zeta_w g \int_{l_c} S_{R(i)} d\xi - 2 \int_{l_c} N_{R(i)} T_{R,1'} d\xi - \int_{l_c} \lambda_{R(i)} \ddot{T}_{R,1''} d\xi \\ &= F_{swR(F)} + F_{swR(D)} + F_{swR(I)} \end{aligned} \quad (8.28)$$

where F_{swR} are the total hydrodynamic forces acting on the starboard sidewall (N) and $F_{swR(F)}$ the buoyancy acting on sidewalls (N):

$$F_{swR(F)} = 0.5\rho_w g \Delta x \left[T_{R1}^2 \sum_{i=1}^n (\tan \beta_{1i} + \tan \beta_{2i}) + 2T_{R1} \sum_{i=1}^n BB_i \right]$$

where n is the number of stations along the craft length, and Δx the space between two stations (m). $F_{swR(D)}$ is the heaving damping force acting on the sidewall (N):

$$\begin{aligned} F_{swR(D)} &= 2\Delta x [\zeta_A \omega \sin(\pi B_c/L_w \cos \theta - \omega t) + \dot{p}_c/2\gamma_w - \dot{\zeta}_g \\ &\quad + (Z_{sw} \sin \theta - 0.5B_c \cos \theta)\dot{\theta}] \sum_{i=1}^n N_{R(i)} \end{aligned} \quad (8.29)$$

$F_{swR(I)}$ is the heave inertia force of added mass acting on the sidewall (N):

$$\begin{aligned} F_{swR(I)} &= 2\Delta x [-\zeta_A \omega^2 \cos(\pi B_c/L_w \cos \theta - \omega t) + \ddot{p}_c/2\gamma_w - \ddot{\zeta}_g \\ &\quad + (Z_{sw} \sin \theta - 0.5B_c \cos \theta)\ddot{\theta}] \sum_{i=1}^n \lambda_{R(i)} \end{aligned} \quad (8.30)$$

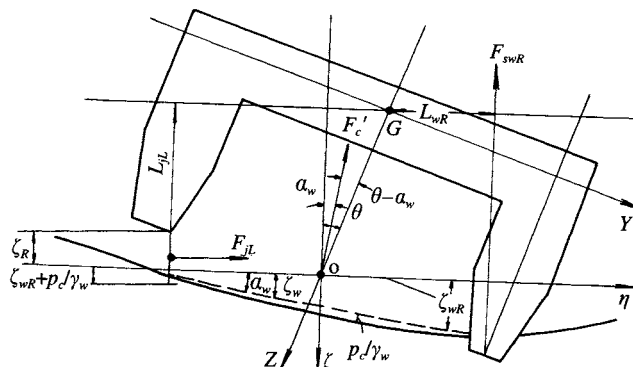


Fig. 8.2 Forces acting on SES when rolling.

$\lambda_{(i)}$, $N_{(i)}$ represent the dimensionless coefficients of heaving damping and added mass for unit length. Considering that the sidewalls are thin and located far from the roll axis, then the coefficients for roll damping and added mass of sidewalls can be obtained approximately by using the heave damping and added mass coefficient of the sidewalls. Therefore the coefficients of heave damping and added mass for conventional ships can be fully used for the calculation, i.e. the experimental results in ref. 80.

During the calculation at MARIC, it was found that the immersion area coefficient of sidewall transverse sections was between 0.6 and 1.0 and $B_n/T_{R,L}$ was about 1.2 where the B_n represented the immersed width of sidewalls and the dimensional coefficient for wave encounter frequency $(\omega_e^2 B_n)/2g = B_n/L_w << 0.2$, where L_w represents wavelength. Taking the immersion coefficients of a sidewall transverse section to be 0.8 and $B_n/T_{R,L} = 1.2$, then the dimensionless coefficients of wave damping and added mass for unit length can be expressed as

$$\begin{aligned}\lambda_{(i)} &= 1.4 - 3.1 (\omega_e^2 B_n)/2g \\ N_{(i)} &= 1.5 (\omega_e^2 B_n)/2g\end{aligned}\quad (8.31)$$

The dimensional coefficient of heaving damping and added mass for unit length of sidewalls can be written as

$$\begin{aligned}\lambda_{(i)} &= \lambda_{0(i)} \rho_w TB^2/8 \\ N_{(i)} &= N_{0(i)} \rho_w g^2/\omega_e^3\end{aligned}\quad (8.32)$$

Case 2: Cushion air leaks under the starboard sidewall and port side is immersed
This can be treated the same as in case 1 above, the roll angle is just reversed.

Case 3: Both port and starboard sidewalls immersed

$$F_{sw} = F_{swR} + F_{swL}$$

Assume that the hydrodynamic force on the sidewalls acts on the interception point of the sidewall centre line with its keel plane, then

$$\begin{aligned}L_{wR} &= 0.5 (B_A + B_S) \cos \theta - Z_{sw} \sin \theta \\ L_{wL} &= 0.5 (B_A + B_S) \cos \theta + Z_{sw} \sin \theta\end{aligned}\quad (8.33)$$

where $L_{wR,L}$ is the hydrodynamic moment arm of the sidewall about the craft CG (m) and B_A the top width of the air cushion (m). Thus the moment of hydrodynamic force acting on the sidewall about the CG of the craft can be expressed as

$$M_{swR,L} = F_{swR,L} L_{wR,L} \quad (8.34)$$

Moment M, due to the air jet from cushion to atmosphere

In this section, swaying motion is temporarily not considered, therefore the jet force will not be included in the equations of motion. However, the moment M_j caused by the jet will be the response to the equations of motion, and for this reason the jet moment can be expressed as

$$\begin{aligned} F_{jL,R} &= \rho_a V_{ib} Q_{eswL,R} = 2l_c p_c \Delta Z_{eL,R} \phi \\ L_{jL,R} &= Z_{sw} \cos \theta - B_c / 2 \sin \theta + 0.5 \Delta Z_{eL} \\ M_{jL,R} &= -F_{jL,R} L_{jL,R} \end{aligned} \quad (8.35)$$

where $F_{jL,R}$ are the forces due to the air jet from the air cushion (N), V_{ib} the jet velocity under the sidewalls (m/s) and ϕ the flow rate coefficient.

The nonlinear differential equations of motion

The coupled roll and heave motion of craft on cushion in beam waves is taken into account in the equation, but the sway motion of craft is not. There are three variables in the motion equations. Considering that the hydrodynamic forces (moments) and the air jet force (moments) acting on the craft are different in different conditions of air leakage under the sidewall, some parameters of the equations can be simplified as follows:

- Both sidewalls are immersed, i.e. $\Delta Z_{eR,L} \leq 0$, then

$$A_R = 1.0 \quad A_L = 1.0 \quad B_j = 0$$

- Port sidewall is immersed, but air leaks under starboard sidewall, namely, $\Delta Z_{eL} \leq 0$, $\Delta Z_{eR} > 0$, then

$$A_R = 0 \quad A_L = 1.0 \quad B_j = 1.0$$

- Air leaks under port sidewall, but starboard sidewall is immersed, i.e. $\Delta Z_{eL} > 0$, $\Delta Z_{eR} \leq 0$, then

$$A_R = 1.0 \quad A_L = 0 \quad B_j = 1.0$$

We can also write

$$\begin{aligned} TT_{R,L1} &= A_{R,L} T_{R,L1} \\ NN_{R,L} &= A_{R,L} N_{R,L} \\ \lambda\lambda_{R,L} &= A_{R,L} \lambda_{R,L} \\ M_{jR,L} &= A_{R,L} B_j M_{jR,L} \end{aligned}$$

where

$$\begin{aligned} N_{R,L} &= \sum_{i=1}^n N_{R,L(i)} \\ \lambda_{R,L} &= \sum_{i=1}^n \lambda_{R,L(i)} \end{aligned}$$

Thus the coupled roll and heave differential equations of motion can be written as

$$[W_l] \begin{bmatrix} \ddot{\zeta}_g \\ \dot{\theta} \end{bmatrix} = \begin{bmatrix} F_c \\ M_c \end{bmatrix} + \begin{bmatrix} F_s \\ M_s \end{bmatrix} + \begin{bmatrix} F_{swR} \\ M_{swR} \end{bmatrix} + \begin{bmatrix} F_{swL} \\ M_{swL} \end{bmatrix} + \begin{bmatrix} 0 \\ M_{jR,L} \end{bmatrix} + \begin{bmatrix} W \\ 0 \end{bmatrix} \quad (8.36)$$

where $[W_l]$ is the matrix for coefficient of inertia force, which can be written as

$$[W] = \begin{bmatrix} w/g & 0 \\ 0 & I_\theta \end{bmatrix}$$

where W is the craft weight (N) and I_θ the moment of inertia of craft in roll (Ns^2m).

The suffixes c, s, sw, j in the matrix represent cushion force (moment), force (moment) acting on the skirt, on sidewalls, of course including the buoyancy, damping and inertia force and jet force (moment) blown under the side hulls respectively.

Based on equations (8.24)–(8.31), the terms in (8.36) can be written as

$$\begin{aligned} F_c &= -p_c S_c \sec(\theta - a_w) \cos a_w \\ F_s &= -p_c/2 (\cot a_1 + \cot a_2) \int_{-Bc/2}^{Bc/2} (|ΔZ_{es}| - ΔZ_{es}) dy \\ F_{swR,L} &= 0.5\rho_w g Δx \left[TT_{R,L1}^2 \sum_{i=1}^n (\tan β_{1i} + \tan β_{2i}) + 2TT_{R,L1} \sum_{i=1}^n BB_i \right] \\ &\quad + 2Δx NN_{R,L} [\zeta_A ω_e \sin(πB_c/L_w \cos θ - / + ω_e t) - ξ_g + p_c/2γ_w \\ &\quad + ḡ(Z_{sw} \sin θ - / + B_c/2 \cos θ)] + Δx λλ_{R,L} [-\zeta_A ω_e^2 \cos(πB_c/L_w \\ &\quad - / + ω_e t) - ξ_g + p_c/2γ_w + ḡ(Z_{sw} \sin θ - B_c/2 \cos θ)] \end{aligned}$$

In this equation R and L correspond to (–) and (+). Thus it can be clearly seen that the first term represents the buoyancy acting on the sidewall, the second the damping force and the third the inertia force.

The equations for the moments are then as follows:

$$\begin{aligned} M_c &= -p_c S_c \sec θ \tan(θ - a_w) \\ M_s &= -p_c/2 (\cot a_1 + \cot a_2) \int_{-Bc/2}^{Bc/2} (|ΔZ_{es}| - ΔZ_{es}) y dy \\ M_{jR} &= ΔZ_{eR} 2 φ p_c l_c L_{jR} \\ M_{jL} &= -ΔZ_{eL} 2 φ p_c l_c L_{jL} \\ L_{jR,L} &= Z_{sw} \cos θ + / - B_c/2 \sin θ + ΔZ_{cR,L} \\ M_{swR,L} &= + / - L_{wR,L} F_{swR,L} \\ L_{wR,L} &= (B_A + B_S)/2 \cos θ - / + Z_{sw} \sin θ \end{aligned}$$

Put $x_1 = t$, $x_2 = ξ_g$, $x_3 = ḡ_g$, $x_4 = θ$, $x_5 = ḡ$ and then the equations for force and moment can be simplified as

$$[A][X] = [\dot{A}] \quad (8.37)$$

where

$$[A] = \begin{bmatrix} a_{11} & a_{12} & a_{13} & a_{14} \\ a_{21} & a_{22} & a_{23} & a_{24} \end{bmatrix}$$

$$[X] = \begin{bmatrix} \dot{x}_3 \\ x_3 \\ \dot{x}_5 \\ x_5 \end{bmatrix}$$

$$[\dot{A}] = \begin{bmatrix} a_{15} \\ a_{25} \end{bmatrix}$$

$$\begin{aligned} a_{11} &= w/g + \Delta x (\lambda\lambda_R + \lambda\lambda_L) \\ a_{12} &= 2\Delta x (NN_R + NN_L) \\ a_{13} &= -\Delta x (\lambda\lambda_R L_{RR} + \lambda\lambda_L L_{LL}) \\ a_{14} &= -2\Delta x (NN_R L_{RR} + NN_L L_{LL}) \\ a_{21} &= \Delta x (\lambda\lambda_R L_{wR} - \lambda\lambda_L L_{wl}) \\ a_{22} &= \Delta x (NN_R L_{wR} - NN_L L_{wl}) \\ a_{23} &= I_\theta + \Delta x (\lambda\lambda_L L_{ll} L_{wl} - \lambda\lambda_R L_{RR} L_{wR}) \\ a_{24} &= 2\Delta x (NN_L L_{ll} L_{wl} - NN_R L_{RR} L_{wR}) \\ a_{15} &= F_c + F_s + F_{BF} + F_p + F_{WA} + W \\ a_{25} &= Mc + Ms + \{M_{BRF} + M_{BLF}\} + \{M_{jJR} + M_{jJL}\} + Mp + M_{WA} \\ L_{RR} &= Z_{sw} \sin \theta - B_c/2 \cos \theta \\ L_{LL} &= Z_{sw} \sin \theta + B_c/2 \cos \theta \end{aligned}$$

and in term a_{15} ,

$$\begin{aligned} F_{BF} &= -0.5\rho_w g \Delta x \left[(TT_{R1}^2 + TT_{L1}^2) \sum_{i=1}^n (\tan \beta_{li} + \tan \beta_{2i}) \right. \\ &\quad \left. + 2 (TT_{R1} + TT_{L1}) \sum_{i=1}^n BB_i \right] \end{aligned}$$

$$\begin{aligned} T_{R,L1} &= -\Delta Z_{eR,L} + p_c/2\gamma_w \\ F_p &= \Delta x/\gamma_w [\dot{p}_c(NN_R + NN_L) + \ddot{p}_c/2 - (\lambda\lambda_R + \lambda\lambda_L)] \\ F_{WA} &= \Delta x \zeta_A \omega_e [2NN_R \sin(\pi B_c/L_w \cos x_4 - \omega_e x_1) \\ &\quad - 2NN_L \sin(\pi B_c/L_w \cos x_4 + \omega_e x_1) \\ &\quad - \lambda\lambda_R \omega_e \cos(\pi B_c/L_w \cos x_4 - \omega_e x_1) \\ &\quad - \lambda\lambda_L \omega_e \cos(\pi B_c/L_w \cos x_4 + \omega_e x_1)] \end{aligned}$$

now, in the term a_{25} ,

$$\begin{aligned} M_{BR,LF} &= -0.5\rho_w g \Delta x L_{wR,L} \left[TT_{R,L1}^2 \sum_{i=1}^n (\tan \beta_{li} + \tan \beta_{2i}) + 2TT_{R,L1} \sum_{i=1}^n BB_i \right] \\ M_p &= \Delta x/\gamma_w [L_{wR} (NN_R \dot{p}_c + \lambda\lambda_R \ddot{p}_c) - L_{wl} (NN_L \dot{p}_c + \lambda\lambda_L \ddot{p}_c/2)] \\ M_{WA} &= \Delta x \zeta_A \omega [L_{wR} [2NN_R \sin(\pi B_c/L_w \cos x_4 - \omega_e x_1) \\ &\quad - \lambda\lambda_R \omega_e \cos(\pi B_c/L_w \cos x_4 - \omega_e x_1)] \end{aligned}$$

$$+ L_{wl} [2NN_L \sin(\pi B_c/L_w \cos x_4 + \omega_e x_1) \\ + \lambda \lambda_L \omega_e \cos(\pi B_c/L_w \cos x_4 + \omega_e x_1)]]$$

Finally, the equation can be written in standard form for numerical solution as follows:

$$D = a_{11} a_{23} - a_{21} a_{13} \\ D_1 = a_{15} - a_{12} x_3 - a_{14} x_5 \\ D_2 = a_{25} - a_{22} x_3 - a_{24} x_5$$

then

$$\dot{x}_1 = 1 \\ \dot{x}_2 = x_3 \\ \dot{x}_3 = (a_{23} D_1 - a_{13} D_2)/D \\ \dot{x}_4 = x_5 \\ \dot{x}_5 = (a_{11} D_2 - a_{21} D_1)/D$$

Initial values can be set as follows, in order to obtain the frequency domain motion response:

$$x_{10} = 0 \quad x_{20} = \zeta_{g0} \quad x_{30} = 0 \quad x_{40} = 0 \quad x_{50} = 0$$

The initial values of cushion pressure can also be given as

$$p_{c0} = p_c \quad \dot{p}_{c0} = 0 \quad \ddot{p}_{c0} = 0$$

Computer program logic for solving the motion equations

A computer program has been developed at MARIC to facilitate numerical solution of the motion equations, as follows:

- First we can calculate from the equilibrium equation the various equilibrium values of craft parameters (Q_0, T_0, P_{c0}) when the craft hovers static on calm water.
- Then we can calculate according to the equilibrium values the initial values of various parameters in the waves.
- Finally we can predict the time-domain motion response by solving the differential equation of motions. These equations can be solved by the Runge–Kutta method, and hence the time-domain motion response obtained from which we can consequently obtain the frequency-domain motion response.

The block diagram for this method of solving the coupled roll and heave differential equations of motion for an SES in beam seas is illustrated in Fig. 8.3. Following each time step p_c is adjusted as follows:

$$p_c^1(t + \Delta t) = p_c(t) + k_c [p_c^{(0)}(t + \Delta t) - p_c(t)] \quad (8.38)$$

During the solution of the differential equations of motion, at first we input the geometric shape and data of the craft into the computer. The initial values of the roll, heave, trim, cushion pressure and vertical height of the CG of the craft running on cushion on calm water can be calculated according to the equilibrium equation of forces (moments) flow rate continuity equation and the characteristic equation for fan and air ducts. If one inputs a given wavelength and height of beam wave, then the differential equation of motion with determined initial values, such as $t_0, \theta_0, \dot{\theta}_0, \zeta_{g0}, \dot{\zeta}_{g0}, p_{c0}, \dot{p}_{c0}, \ddot{p}_{c0}$ can be solved by iteration.

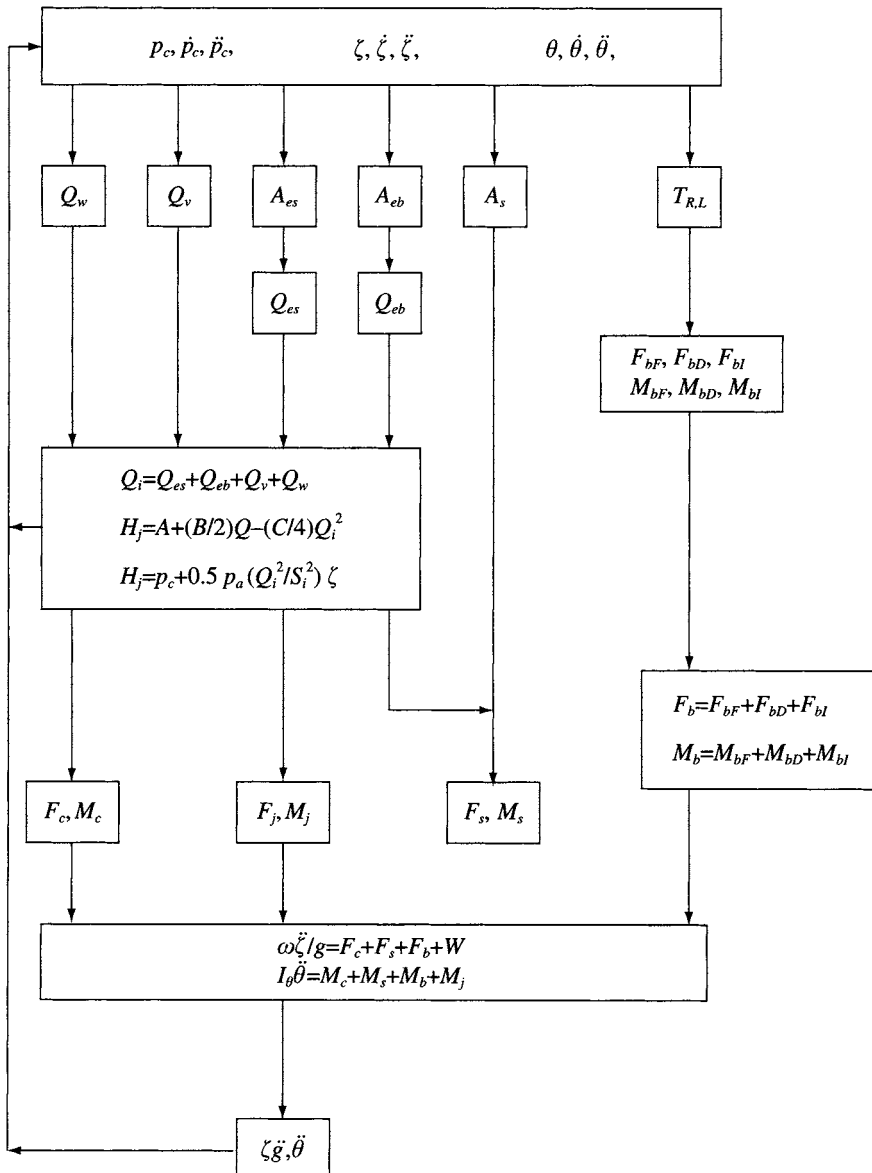


Fig. 8.3 Block diagram for solving the differential equations of coupled roll and heave motion of SES in beam seas.

Comparison of calculation results with experiments

The calculation and experiments of coupled roll and heave motion of steel hull SES version 719 in beam seas has been carried out in the case where the fan flow rate was small.

Tests showed that in the case of large fan flow rate, a large amount of cushion air

would be blown out under the sidewall. This led to a self-excitation of vibration, because the frequency of exciting force due to the jet air blown under the sidewalls was very close to the roll frequency, consequently a 'beat' occurred in the roll motion of the model. Owing to the complicated physical and mathematical model of the beat motion mentioned above, MARIC have not yet solved this problem.

The coupled roll and heave motion of model craft 719 (scale ratio $\gamma = 1:12$) in beam waves and its frequency-domain motion response have been predicted using the iterative method by computer. During calculation, the parameters of the craft and waves were given as follows:

$$\begin{aligned} \text{Dimensionless mass of the model craft: } \bar{m} &= m/(\rho_w L_c^3) = 0.0048 \\ \text{Cushion length beam ratio: } L_c/B_c &= 4 \\ \text{Dimensionless wave height: } \zeta_a/B_c &= 0.0191 \sim 0.0281 \\ \text{Dimensionless wavelength: } L_w/B_c &= 2.2 \sim 7.6 \end{aligned}$$

Experiments with the model in static hovering mode in beam waves in the towing tank were carried out and comparisons of the theoretical prediction for vertical acceleration at the CG and roll motion amplitude of the model were made with experimental results in the frequency domain.

The responses are shown in Figs 8.4 and 8.5 respectively. One can see that a peak value at $\omega_e = 5$ in Fig. 8.5 can be found both in theoretical and experimental results. This can be considered the natural frequency of roll for the model. The average value of cushion pressure and its amplitude fluctuation in frequency domain response are shown in Figs 8.6(a) and (b). It is found that the calculated results are close to those obtained from model experiments, both having the same trend.

Further investigations required

1. In the case where the wavelengths are longer, due to the extreme fluctuation of cushion pressure, it is difficult to solve the differential equation of motions due to divergence of the calculation. It is suggested this calculation method be improved.

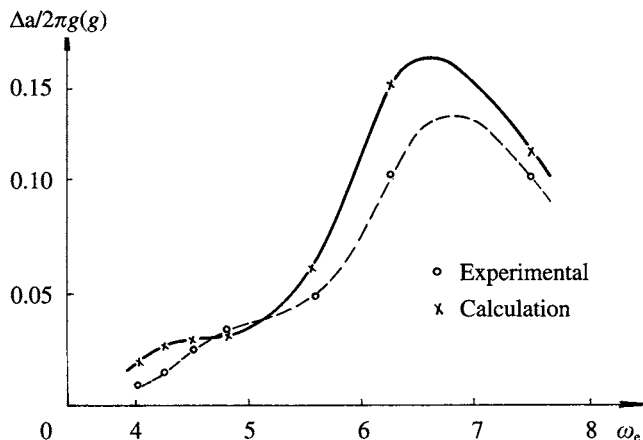


Fig. 8.4 Frequency response curves for heave acceleration at SES model CG in beam seas.

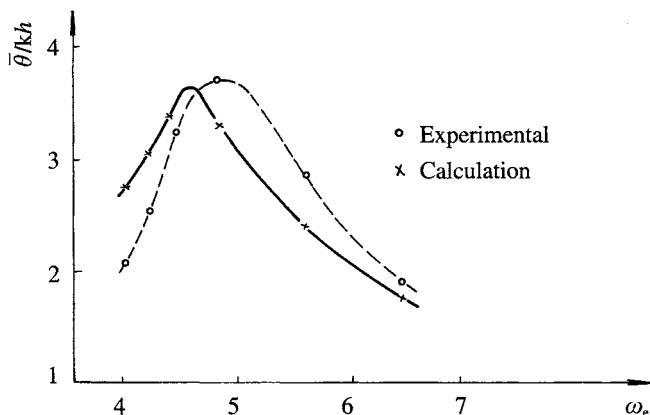


Fig. 8.5 Frequency response curves for the roll amplitude of an SES model in beam seas.

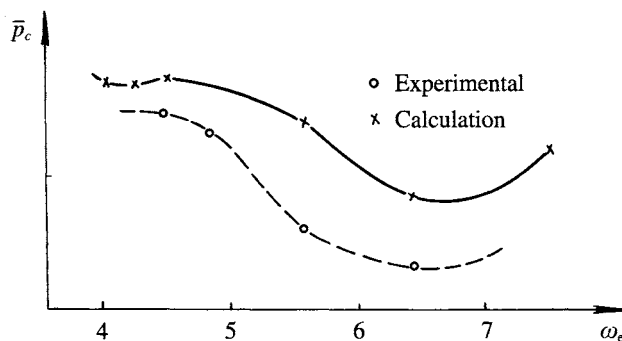


Fig. 8.6(a) Frequency response curves for the mean cushion pressure of an SES model in beam seas.

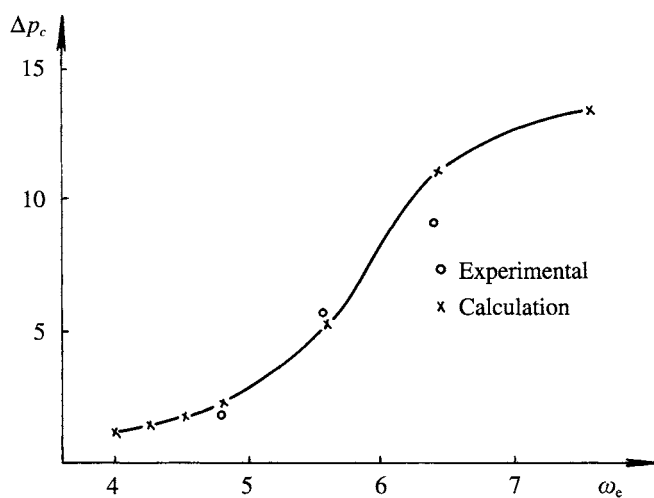


Fig. 8.6(b) Frequency response curves for the cushion pressure fluctuation of the SES model in beam seas.

2. The 'beat' phenomenon in roll of model craft with large air inflow rate can be found in the experiments. It is suggested that the air jet disturbance factor may be enhanced in such a case and cause the 'beat' phenomenon because the frequency of jet disturbance is close to the roll frequency with a little phase lag. Hence the rationale of such a physical phenomenon has to be investigated in order to obtain a more precise mathematical model for calculation.
3. Damping force and added mass due to the combined action of air cushion and sidewalls have not yet been considered in the calculation above, therefore this should be investigated in further research work.
4. Coupled roll and heave motion for small angles is derived in this chapter. In practice the motion to larger craft roll angles in waves is more important when considering craft stability from the safety viewpoint. Hence coupled motion to large rolling angles both for theoretical and test work needs to be investigated in the future.

8.3 Longitudinal SES motions in waves

In section 8.1, we introduced the seaworthiness studies of hovercraft by experts from various countries. The investigations concentrated mainly on the longitudinal (pitch) motions of ACV/SES in waves, as in refs 11, 67 to 69/71, 73 etc. These research papers present differing approaches and analytical methodology.

In this section, the various nonlinear factors associated with motion of a craft running in waves will be discussed. Skirt contact with the water makes the forces acting on the craft have strong nonlinear characteristics. From Fig. 8.7 one can see that hydrodynamic forces acting on the skirt vary sharply. It would be convenient if such conditions could be expressed in a simple manner by deriving nonlinear motion equations.

Although the restoring moment of craft is linear when the craft pitches at a small angle (Fig. 8.8), the longitudinal restoring moment increases sharply when the craft

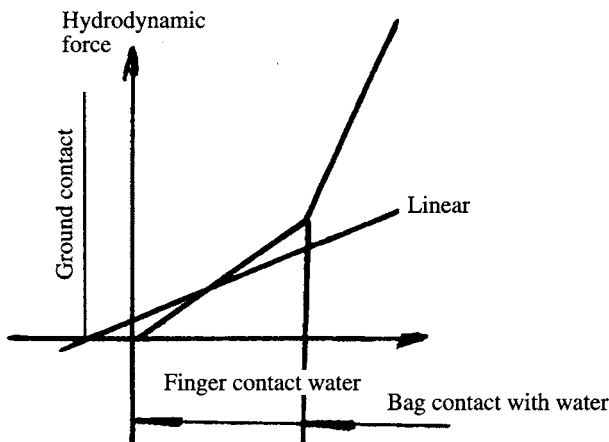


Fig. 8.7 The non-linear characteristics for hydrodynamic forces acting on skirts.

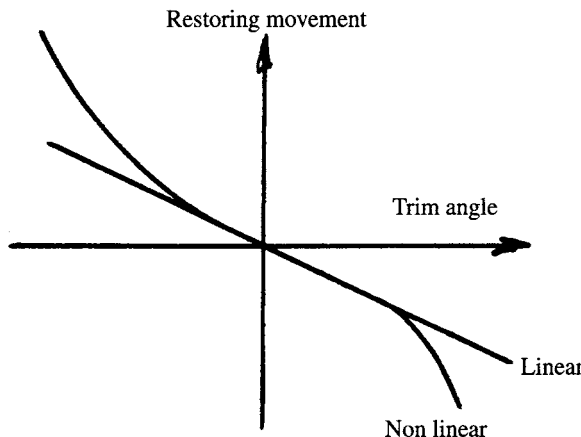


Fig. 8.8 The non-linear characteristics for transverse righting moment on hovercraft.

pitches at a large angle. So it is difficult to analyse such nonlinear characteristics by means of linear equations with adjusted coefficients. However, by applying nonlinear motion equations, the instantaneous restoring moment due to wet skirt hydrodynamic forces can be calculated. This method is more practical and convenient.

Cushion force is not only affected by skirt contact with water but also the non-linearity of fan characteristics. Fan characteristic curves as well as the characteristics of air ducts are parabolic of second order. The slope of the fan characteristic curve sharply affects stability and damping of an air cushion system. In the linear equations of motion, we assume the working point of the fan is constant, which means the slope of the fan characteristic curve stays constant. This will lead to large errors when the craft is running in high seas and the vertical motion of the craft is very large.

In such a case, we can consider air leakage gap, air cushion pressure and air flow rate as functions of time in the nonlinear equations of motion. By this means we can account for the effect of fan characteristics on damping and stability of the air cushion system. Figure 8.9 shows that the change of the curve slope is very large when the fan is operated at larger (or smaller) flow and negative flow rate. Therefore it is more convenient for us to predict craft motion response by means of nonlinear motion equations.

The nonlinearity of the hydrodynamic forces acting on sidewalls arises from the change of draft on each section along the longitudinal craft axis. Particularly when the craft is running in high seas, wave perturbations on the craft are severe and this causes local air leakage under the sidewalls. This results in nonlinearity of sidewall force and air cushion force.

In the derivation of the linear equations of motion, one assumes that the derivatives of the longitudinal stability of the sidewalls are a function of the craft in static equilibrium, in which the effect of air leakage under the sidewalls on craft motion is not taken into account, so that method applies only to the case of small perturbation. However, it would be easier if each effect is considered by the use of nonlinear equations of motion as outlined here.

When a hovercraft is running in heavy seas, it also experiences various physical phenomena such as fan reverse flow, negative air cushion pressure, wave impact on skirt

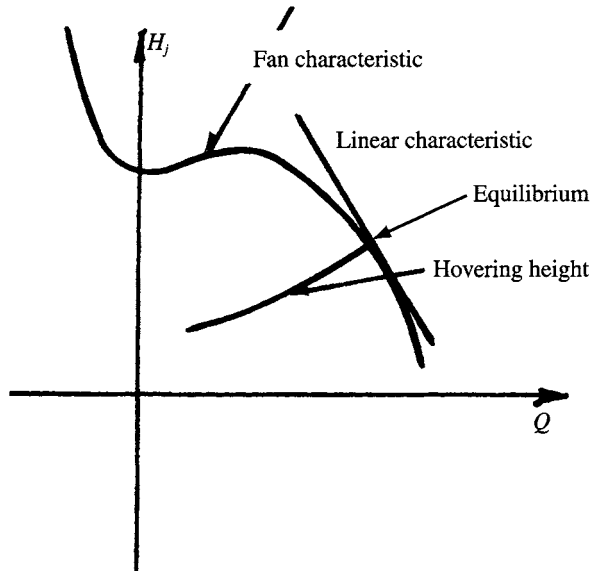


Fig. 8.9 The non-linear characteristics for pressure-flow of lift fans on hovercraft.

fingers or bag, air leakage under sidewalls, etc. One can analyse such phenomena with the aid of non-linear motion equations.

The following principal assumptions are made in order to form nonlinear motion equations:

1. The Froude–Krilov hypothesis is satisfied, which means that waves are not interfered by craft. The effect of sidewalls and skirts on waves and the effect of the air cushion on the surface deformation of waves, are neglected.
2. Uniform distribution of cushion pressure is assumed and the cushion plane is simplified as a rectangle.
3. Changes of air density and cushion pressure in the plenum chamber (air cushion) are considered to be adiabatic, but the outflow of cushion air into the atmosphere incompressible.
4. Fan speed is kept constant and the effect of dynamic response of the fan neglected.
5. Effect of skirt deformation on motions of craft is neglected.
6. Added mass and added mass moment are not taken into account in the equation.
7. The effect of external air dynamic force on the motion of craft is neglected.
8. Bow skirt fingers are regarded as absolutely flexible.
9. Effect of stiffness of stern bag on hydrodynamic forces acting on skirt is taken into account.
10. Cross-section of sidewalls is taken to be a trapezoid to simplify the calculation.

The solution logic is similar to that for solving the coupled roll and heave equations of motion as shown in Fig. 8.10. The calculation in detail can be described as follows [69].

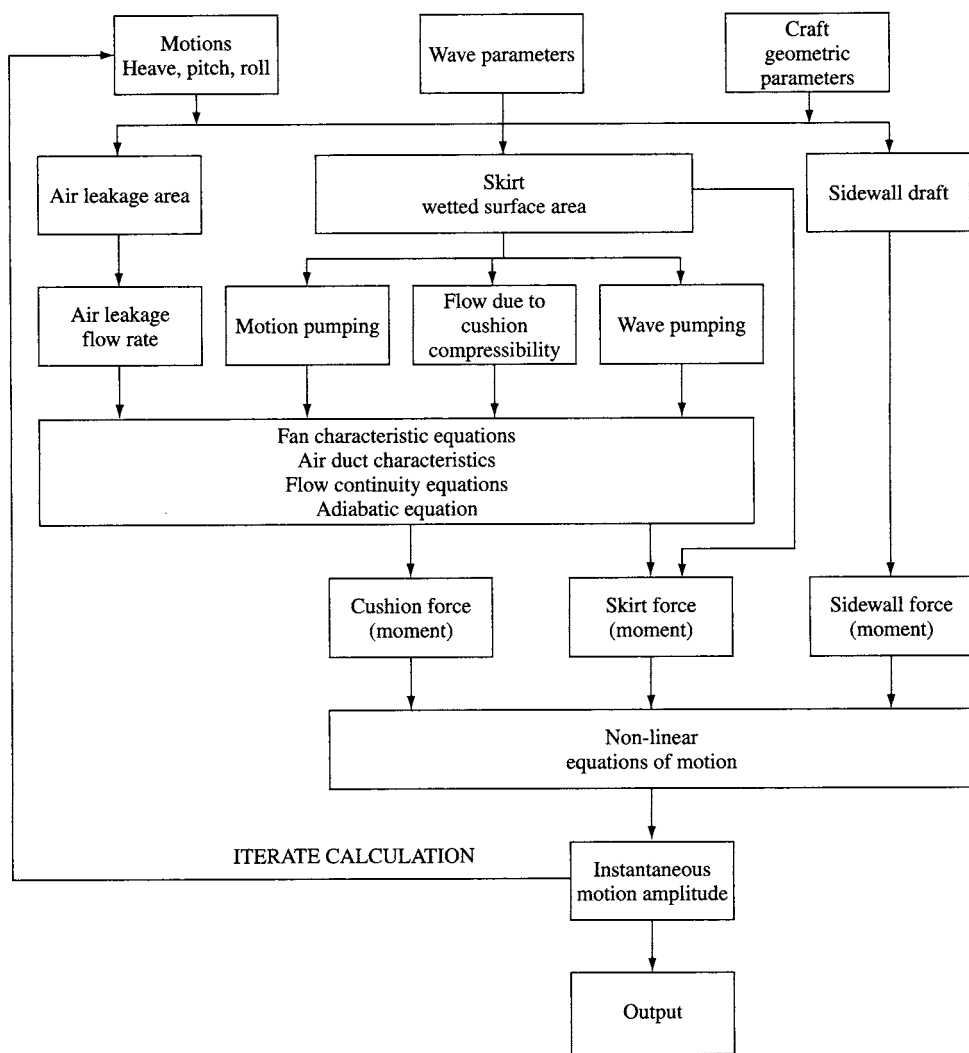


Fig. 8.10 Block diagram for solving SES non-linear differential equations of longitudinal motion in waves.

Coordinate system and geometrical dimensions of craft

Similar to section 8.2, the coordinate system $GXYZ$ fixed on the craft is chosen to be a right-hand coordinate system. The origin point is taken to go through the CG of the craft, GX is a longitudinal axis parallel to the base-line of the sidewall and the forward direction of the craft motion is positive. Along axis GY the starboard direction is positive and axis GZ is perpendicular to the GXY plane and its downward direction is taken to be positive. The outline of the craft is shown in Fig. 8.11 and the configuration of the cushion plane can be simplified as a rectangle with length of L_c , width B_c and area of A_c . There are no compartments in the cushion.

The other geometrical dimensions are illustrated as follows:

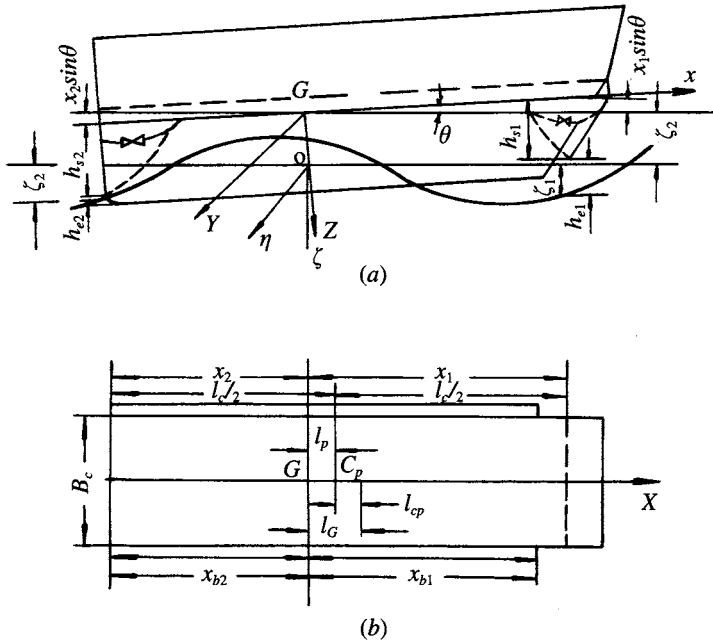


Fig. 8.11 Principal parameters for determining the longitudinal motion of SES in waves.

C_p	Position of pressure centre of air cushion
l_p	Longitudinal distance from CG to C_p (m)
l_G	Longitudinal distance from CG to mid-section (m)
l_{cp}	Longitudinal distance from C_p to midsection, i.e. $l_{cp} = l_G - l_p$ (m)
h_{s1}, h_{s2}	Vertical distances from craft longitudinal axis to lower tips of bow and stern skirt (m)
x_1, x_2	Longitudinal coordinates (on axis GX) of the lower tips of bow and stern skirt respectively; this can be written as

$$x_1 = l_c/2 + l_p \quad (8.39)$$

$$x_2 = -l_c/2 + l_p \quad (8.40)$$

X_{b1}, X_{b2}	Longitudinal GX axis coordinates of sidewall at bow/stern lower tips (m)
h_b	Vertical distance from CG to the base-line of sidewall (m)
ζ_g	Height of CG with respect to the absolute coordinate (m)
ψ	Pitch angle (bow up positive) (°)

Wave equation

With respect to the fixed absolute coordinates $0\xi\eta\zeta$ the equation for two-dimensional waves is given as follows:

$$\zeta_w = \zeta_a \sin (\pm K_w \zeta + \omega t) \quad (8.41)$$

or

$$\zeta_w = \zeta_a \sin (\pm K_w x + \omega_e t) \quad (8.42)$$

where K_w , the wave number, can be written as

$$K_w = 2\pi/L_w \quad (8.43)$$

and ω , the wave frequency, can be written as

$$\omega = [2\pi g/L_w]^{0.5} \quad (8.44)$$

where L_w is the wave length (m), ζ_a the wave amplitude (m) and ω_e the wave encounter frequency (rad/s), which can be written as

$$\omega_e = \omega (1 \pm \omega V_s/g) \quad (8.45)$$

where V_s is the craft speed (m/s).

(In this equation, we take the craft in a head wave as positive and negative in a following wave.) ζ_w is the wave elevation at the distance of x from the CG (m).

For reasons of simplification we take (cf. equation 8.43)

$$K = \pm 2\pi/L_w \quad (8.46)$$

Then the equation of the wave surface can be written as (cf. equation 8.42)

$$\zeta_w = \zeta_a \sin (Kx + \omega_e t) \quad (8.47)$$

The vertical velocity of wave motion and wave slope can be expressed as

$$\dot{\zeta}_w = \zeta_a \omega_e \cos (Kx + \omega_e t) \quad (8.48)$$

$$a_w = \frac{\partial \zeta_w}{\partial x} = K \zeta_a \cos (Kx + \omega_e t) \quad (8.49)$$

where $\dot{\zeta}_w$ is the vertical velocity of wave motion (m/s) and a_w the wave slope (°).

Then the wave elevation, vertical velocity of wave and wave slope at the CG are expressed by:

$$\begin{aligned} \zeta_{wg} &= \zeta_a \sin \omega_e t \\ \dot{\zeta}_{wg} &= \zeta_a \cos \omega_e t \\ a_{wg} &= K \zeta_a \cos \omega_e t \end{aligned} \quad (8.50)$$

The wave elevation, under the bow/stern skirt ζ_{w1} , ζ_{w2} , and wave slope a_{w1} , a_{w2} , can be expressed as

$$\begin{aligned} \zeta_{w1} &= \zeta_a \sin (Kx_1 + \omega_e t) \\ \zeta_{w2} &= \zeta_a \sin (Kx_2 + \omega_e t) \\ a_{w1} &= K \zeta_a \omega_e \cos (Kx_1 + \omega_e t) \\ a_{w2} &= K \zeta_a \omega_e \cos (Kx_2 + \omega_e t) \end{aligned} \quad (8.51)$$

Here suffixes 1 and 2 represent the position at the bow and stern.

Air cushion system

As for the case of uniform distribution of air cushion pressure, air cushion force and moment can be expressed as

$$F_c = -p_c A_c \cos \psi$$

$$M_c = p_c A_c L_p \quad (8.52)$$

Cushion pressure can be obtained by solving the equations of fan and duct characteristics as well as the equation of continuity flow, which is expressed as

$$Q_i = Q_e + \frac{1}{\rho_a} \frac{d}{dt} (\rho_a V_c) \quad (8.53)$$

where Q_i is the inflow rate of fan (m^3/s), Q_e the flow rate of air leakage (m^3/s) and V_c the cushion volume (m^3). The second term on the right of equation (8.53) represents the change of flow rate with respect to volume and density of air cushion, i.e. the sum of flow rate with respect to wave pumping, motion pumping of the craft and compressibility of the air cushion.

The flow rate of air leakage Q_e

$$Q_e = Q_{e1} + Q_{e2} + Q_{eb} \quad (8.54)$$

where Q_{e1} is the flow rate of air leakage under the bow skirt,

$$Q_{e1} = \phi_{s1} V_c A_{e1} \quad (8.55a)$$

Q_{e2} is the flow rate of air leakage under the stern skirt,

$$Q_{e2} = \phi_{s2} V_c A_{e2} \quad (8.55b)$$

and Q_{eb} is the flow rate of air leakage under the sidewall,

$$Q_{eb} = \phi_{eb} V_c A_{eb} \quad (8.55c)$$

ϕ_{s1} , ϕ_{s2} and ϕ_{eb} represent the coefficient of flow rate under the bow skirt, stern skirt and sidewall respectively.

$$A_{e1} = \begin{cases} B_c h_{e1} & \text{when } h_{e1} > 0 \\ 0 & \text{when } h_{e1} \leq 0 \end{cases} \quad (8.56)$$

$$A_{e2} = \begin{cases} B_c h_{e2} & \text{when } h_{e2} > 0 \\ 0 & \text{when } h_{e2} \leq 0 \end{cases} \quad (8.57)$$

where h_{e1} is the height of air leakage under the bow skirt and can be written as

$$h_{e1} = -\zeta_g + x_1 \sin \psi - h_{s1} \cos \psi + \zeta_{w1} \quad (8.58a)$$

and h_{e2} the height of leakage under the stern skirt, can be written as

$$h_{e2} = -\zeta_g + x_2 \sin \psi - h_{s2} \cos \psi + \zeta_{w1} \quad (8.58b)$$

where h_{s1} and h_{s2} are vertical distance between the CG and the lower tip of the stern skirt.

To simplify the calculation, equation (8.57) may be written as

$$A_{e1} = B_c (h_{e1} + |h_{e1}|)/2$$

$$A_{e2} = B_c (h_{e2} + |h_{e2}|)/2 \quad (8.59)$$

The flow rate due to mass change rate of air cushion

$$\frac{1}{\rho_a} \frac{d}{dt} (\rho_a V_c) = \dot{V}_c + \frac{V_c}{\rho_a} \dot{\rho}_a \quad (8.60)$$

where \dot{V}_c is the flow rate due to the wave pumping and motion pumping of the craft, i.e. the flow rate due to the rate of change of cushion volume of craft moving in waves, Q_w , and $(V_c/\rho_a)\dot{\rho}_a$ the flow rate due to the change of density of cushion air (Q_v), i.e. due to the compressibility of the air cushion. In this case, we assume the change of air density in the cushion depends upon the law of adiabatic change and the air density in the air cushion at the static hovering condition is equal to that in atmosphere, then Q_v can be written as (assume the adiabatic coefficient $r = 1.4$)

$$Q_v = V_c \dot{\rho}_a / (1.4 (p_c + p_a)) \quad (8.61)$$

$$V_c = B_c \int_{x_2}^{x_1} h_v(x) dx$$

where $h_v(x)$ is the depth of air cushion and can be written as

$$h_v(x) = -\zeta_g + x \sin \psi - h_{b0} \cos \psi + \zeta_w(x)$$

where h_{b0} is the vertical distance from the CG to the bottom of the craft along axis CZ . Thus

$$\dot{V}_c = \int_{x_2}^{x_1} (-\dot{\zeta}_g + x_c \cos \psi - \dot{\psi} + \dot{\zeta}_w) B_c dx = Q_w$$

If we integrate this expression, then

$$Q_w = (-\dot{\zeta}_g + L_p \cos \psi - \dot{\psi}) A_c + \sin C_w / C_w A_c \omega_e \zeta_a \cos (KL_p + \omega_e t) \quad (8.62)$$

The first term on the right of the equation represents the flow rate due to the motion pumping of the craft and the second term represents the flow rate due to the wave pumping where

$$C_w = \pi L_c / L_w$$

Hydrodynamic forces acting on skirts

The bow skirt is assumed to be of the bag and finger type and the stern skirt of the multiple bag type. Fingers of the bow skirt are assumed to be absolutely flexible and the skirt finger will deflect as soon as it comes into contact with the water.

We consider that the hydrodynamic force acting on skirts consists of two parts. One is due to cushion pressure or bag pressure, equal to the air cushion force acting on the wetted surface before deflection. Its vertical component is the lift due to the increase in cushion area while its horizontal component is equal to the product of cushion pressure and projected area of wetted surface on the vertical plane. The second part is due to water friction. Fingers, where in contact with and subsequently lying on the waves, induce water friction force, the direction of which is parallel to the wave surface. This force is divided into vertical and horizontal components. The bow skirt bag may be impacted by waves and local deflection will take place. In that case

cushion pressure has to be altered by bag pressure in the calculation of the hydrodynamic force of the skirt bag.

Assume A_{sf} , A_{st} are the wetted area of the fingers and bag and of the skirt bag respectively. Suffix k represents projection on the vertical plane and h_{sf} represents finger height (Fig. 8.12), in the case that the fingers of the bow skirt are immersed, but the bow skirt bag is not, i.e. while $h_{el} < 0$ and $|h_{el}| < h_{sf}$ then

$$A_{sfk} = A_{el} - B_c h_{el} \quad \text{and} \quad A_{stk} = 0$$

where A_{sfk} is the projected area of the wetted surface in the vertical plane and h_{el} the immersed height of the bow finger, or the bow finger and bag. Thus the wetted area of fingers A_{sf} can be written as

$$A_{sf} = A_{sfk} / \sin(a_1 + \psi) \quad (8.63)$$

where a_1 is the inclination angle of the skirt with respect to axis GX .

When $h_{el} < 0$ and $|h_{el}| > h_{sf}$ (i.e. bag immersed), then

$$\begin{aligned} A_{sl} &= A_{sf} + A_{st} \\ &= B_c h_{sf} / \sin(a_1 + \psi) + B_c (-h_{el} - h_{sf}) / \sin(a_1 + \psi) \end{aligned} \quad (8.64)$$

where A_{sl} is the total wetted surface of the bow skirt.

Here the vertical hydrodynamic force acting on the bow skirt F_{sr} can be written as follows:

$$F_{rl} = -(p_c A_{sfk} + p_{tl} A_{stk}) / \tan(a_1 + \psi) - R_F A_{sl} \sin a_{wl} \quad (8.65)$$

where a_w is the wave slope ($^{\circ}$) and R_F the water friction force per unit area of skirt, which can be written as

$$R_F = C_f \times 0.5 \rho_w V_s^2$$

where C_f is the coefficient of friction. Thus the total hydrodynamic drag of bow skirts can be written as:

$$R_{sl} = p_c A_{sfk} + p_{tl} A_{stk} + R_F A_{sl} \cos a_{wl} \quad (8.66)$$

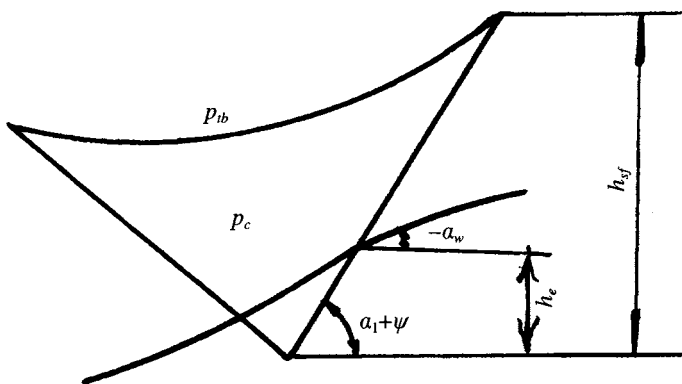


Fig. 8.12 Sketch for submergence of bow skirt.

For the same reason, the hydrodynamic forces acting on the stern seal are

$$\begin{aligned} F_{s2} &= -(C_{ps} p_{12} A_{sk})/\tan(a_2 + \psi) - R_F A_{s2} \sin a_{w2} \\ R_{s2} &= C_{ps} p_{12} A_{sk} + R_F A_{s2} \cos a_{w2} \end{aligned} \quad (8.67)$$

where F_s is the vertical hydrodynamic force acting on the stern seal, R_s the hydrodynamic drag acting on the stern seal, p_{12} the stern bag pressure and C_{ps} the coefficient with respect to the stiffness of the bag obtained from experiments.

The sum of moments induced by vertical forces and drag about the CG can be written as

$$\begin{aligned} F_s &= F_{s1} + F_{s2} \\ R_s &= R_{s1} + R_{s2} \\ M_s &= F_{s1}(x_1 \cos \psi + R_{hs1} \sin \psi) - F_{s2}(x_2 \cos \psi + R_{hs2} \sin \psi) \\ &\quad + R_{s1}(x_1 \sin \psi - R_{hs1} \cos \psi) + R_{s2}(x_2 \sin \psi - R_{hs2} \cos \psi) \end{aligned} \quad (8.68)$$

where F_s is the sum of vertical forces acting on the bow and stern skirts (N), R_s the sum of water drag forces acting on the bow and stern skirts (N), M_s the sum of hydrodynamic moments acting on the bow and stern skirt about the CG (Nm) and R_{hs1} , R_{hs2} are the vertical distances between the axis GX and the points on the bow and stern skirts which are under the action of the hydrodynamic forces and can be written as

$$\begin{aligned} R_{hs1} &= h_{s1} + h_{e1}/2 \\ R_{hs2} &= h_{s2} + h_{e2}/2 \end{aligned}$$

Hydrodynamic forces and moments acting on sidewalls

The configuration of sidewalls can be simplified as shown in Fig. 8.13. The draft h_T , buoyancy of sidewalls D_b and the restoring moment supplied by the buoyancy, M_D can be written respectively as

$$h_T = h_b \cos \psi + \zeta_g - x \sin \psi - \zeta_w \quad (8.69)$$

$$\begin{aligned} D_b &= -\rho_w g \int_{xb2}^{xb1} [((h_T + |h_T|)/2)^2 (\tan \theta_{b1} + \tan \theta_{b2}) + (h_T + |h_T|) B_2] dx \\ M_D &= \rho_w g \int_{xb2}^{xb1} [((h_T + |h_T|)/2)^2 (\tan \theta_{b1} + \tan \theta_{b2}) + (h_T + |h_T|) B_2] X dx \end{aligned} \quad (8.70)$$

where the geometrical parameters $\bar{B}B_1$, $\bar{B}B_2$, θ_{b1} , θ_{b2} are shown in Fig. 8.13.

The outflow rate under the sidewalls can be expressed by

$$Q_{eb} = 2\phi_{eb} V_e \int_{Xb2}^{Xb1} (-h_T + |h_T|)/2 dx \quad (8.71)$$

in which ϕ_{eb} , the coefficient of air flow leaked under the sidewall with respect to the wave damping force and added mass induced by the sidewall-air cushion system, can be obtained by experiments as in the introduction to this chapter in section 8.2.

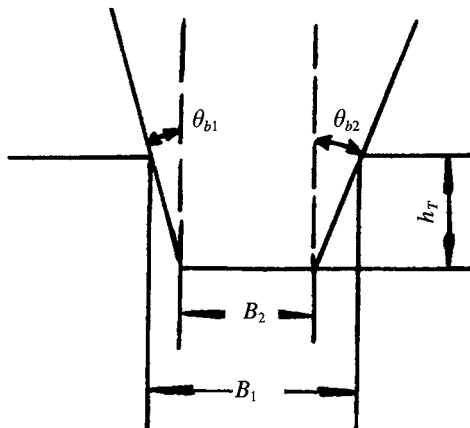


Fig. 8.13 Transverse section of sidewall.

The nonlinear differential equations of motion

The coupled pitch and heave nonlinear differential equations of motion can be written as

$$[W_I] \begin{bmatrix} \ddot{\zeta}_g \\ \dot{\psi} \end{bmatrix} = \begin{bmatrix} F_C \\ M_C \end{bmatrix} + \begin{bmatrix} F_s \\ M_s \end{bmatrix} + \begin{bmatrix} F_b \\ M_b \end{bmatrix} + \begin{bmatrix} W \\ M_0 \end{bmatrix} \quad (8.72)$$

in which

$$W_I = \begin{bmatrix} W/g & 0 \\ 0 & I_\psi \end{bmatrix}$$

where M_0 are the moments of both drag and thrust about the CG of craft running at given speed and I_ψ the pitch moment of inertia of the craft.

Solution of equations and comparison with experiments

Similar to the procedure described in section 8.2, the coupled pitch and heave are nonlinear differential equations which can be solved with the aid of computers, the block diagram for which is shown in Fig. 8.14.

A comparison of theoretical predictions with experiments in the frequency domain response is made below:

1. The test model is model 719 and its non-dimensional coefficients are the same as that in section 8.2, the wave parameters can be obtained as

$$\zeta_a/L_c \text{ (non-dimensional wave height)} = 0.025$$

$$L_w/L_c \text{ (non-dimensional wavelength)} = 1.0 - 7.5$$

The tests were carried out in a towing tank of MARIC (test in head waves).

2. Figure 8.15(a) shows the response of heave motion; it is found that the maximum value of response does not exceed unity because of the high damping coefficient of

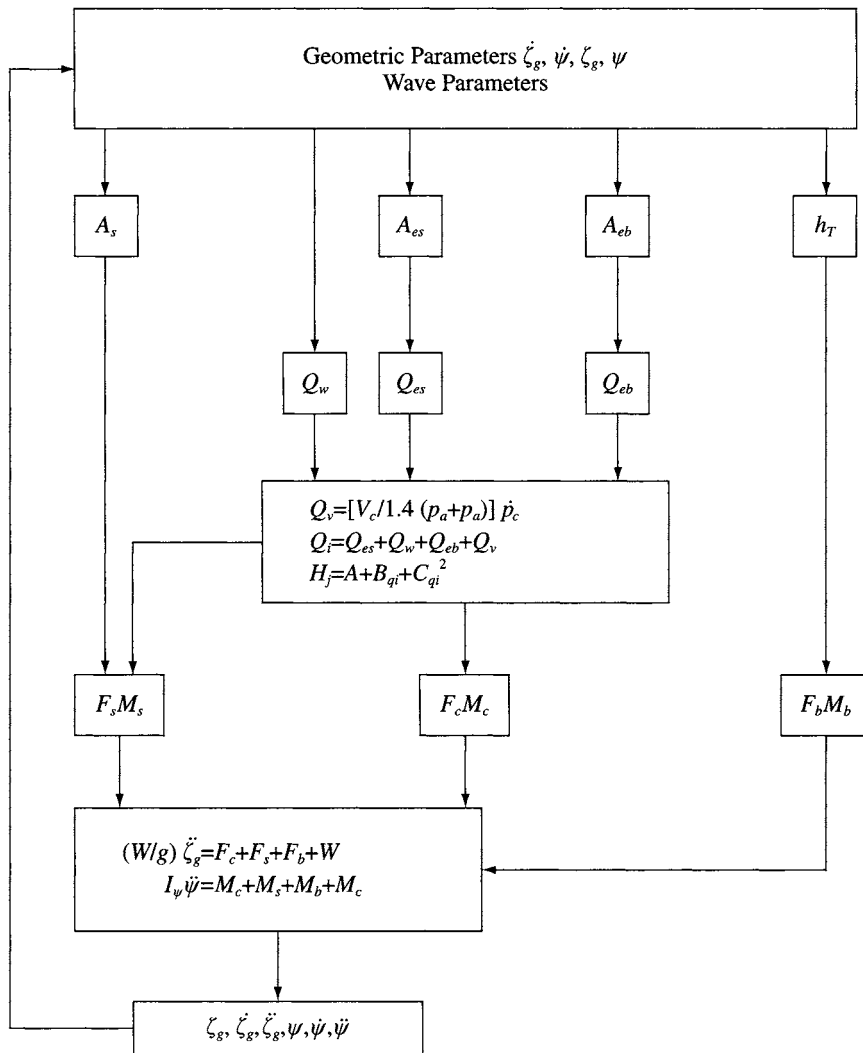


Fig. 8.14 Block diagram for solving the differential equations of longitudinal motion of SES in waves.

motion. It is noted that the heave response depends strongly upon the cushion system characteristics. The calculated values are larger than the experimental results, but both have the same trend. The figure shows a small step at the point corresponding to non-dimensional frequency of 4 due to the coupled pitch–heave motion and wave pumping. The figure also shows a peak at higher frequency, where the wavelength is approximately equal to the craft length.

Figure 8.15(b) indicates that the perturbation force of the wave, the peak of which corresponds to the peak of heave response, has a strong influence on the heave motion response. The response indicates that the heave motion has high heave stability and damping.

3. Figure 8.16 shows the pitch response ψ_{ζ_a} to the wave amplitude as it varies with

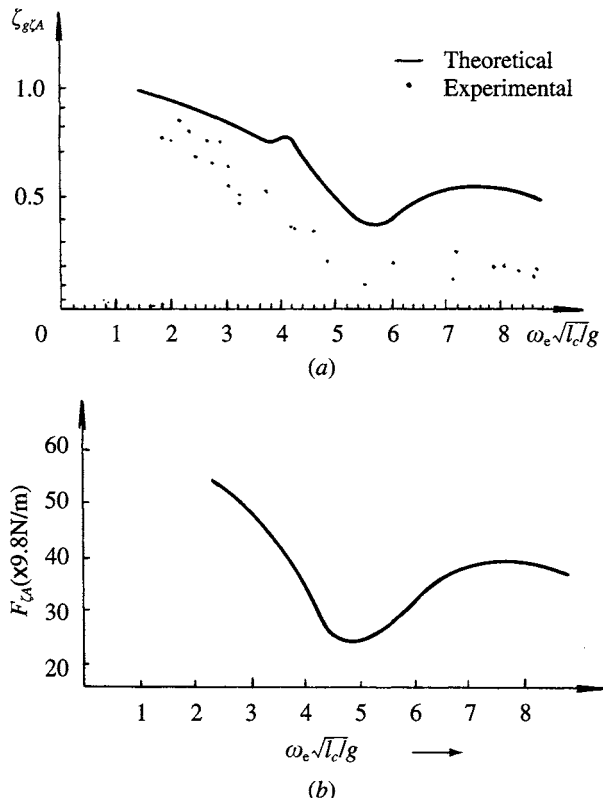


Fig. 8.15 Unit (response/m waveheight) frequency response for heave motion: (a) frequency response for heave amplitude; (b) frequency response for heaving exciting force.

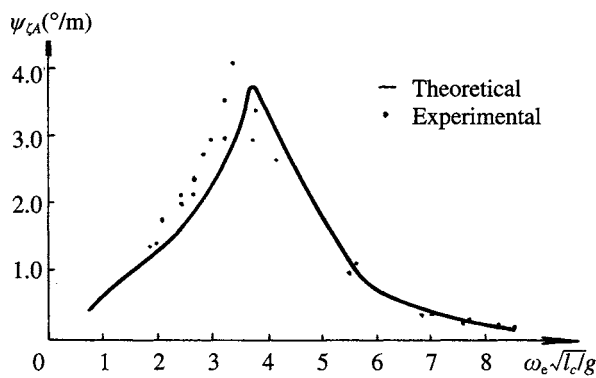


Fig. 8.16 Unit frequency response for pitch angle of SES in waves.

encounter frequency. It is shown that the theoretical prediction is close to the experimental results. Figure 8.17 gives the pitch perturbation moment. It may be noticed that the peak is at the point of non-dimensional frequency of 4, at which the wavelength is about twice the craft length and so the wave perturbation

moment is maximum. To sum up, the peak at about non-dimensional frequency of 4 is due to pitch and heave motion and the peak at higher frequency is due to heave perturbation. The peak on the pitch response curve is rather steep, which shows that the pitch moment has low damping .

- Figure 8.18 shows the bow acceleration response. The peak at non-dimensional frequency of 4 is induced by both heave and pitch motion. Due to the vertical acceleration of the craft increasing in square proportion with encounter frequency, the vertical acceleration of the craft increases rapidly. The hollow on the curve is due to the superposition of hollows caused by both heave and pitch motion.

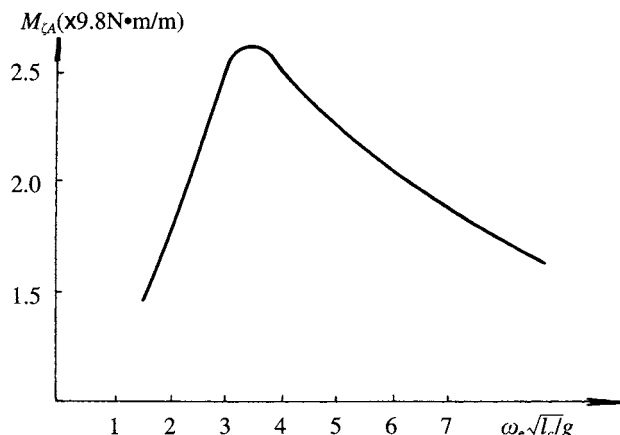


Fig. 8.17 Unit frequency response for pitch exciting moment.

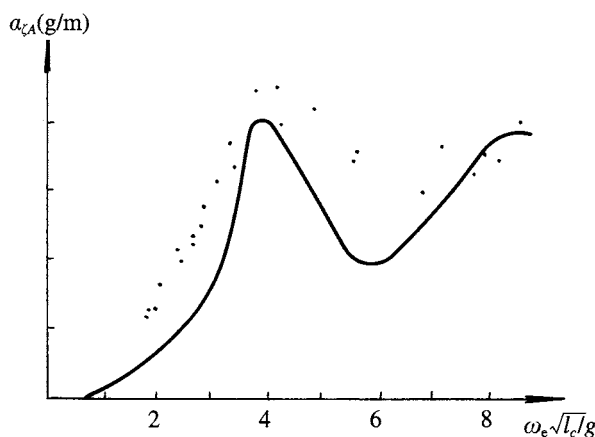


Fig. 8.18 Unit frequency response of bow acceleration for SES in head seas.

8.4 Longitudinal motions of an ACV in regular waves

Seaworthiness motions analysis of ACVs is similar to that of SESs. In this section, we will introduce the linear differential equations of motion for an ACV in regular waves. As mentioned above, although this method is rather artificial, the results obtained by this method are more directly understood and so one can estimate the effect of changes in various parameters of the linear differential equations of motion.

For a typical ACV, the cushion moment will be the predominant restoring moment due to the cushion compartmentation or skirt of deformation. It is normally possible to neglect the effect of hydrodynamic force (moment) acting on the skirt. References 11, 67 and 71 discussed this subject with respect to the linear equations of motion. Here we introduce the linear equations concerning coupled heave and pitch motion [70]. In this approach the hydrodynamic force (moment) acting on the skirt and the wave surface deformation due to the motion of cushion air are not considered, but we take the Froude–Krilov hypothesis and effect of cushion air compressibility into account.

In the course of deriving the equations, one still adopts the assumptions in section 8.3 above, namely recognizing the Froude–Krilov hypothesis; simplifying the cushion plane as a rectangle; taking the change of pressure and density in the air cushion to comply with the adiabatic principle; neglecting the dynamic response of air cushion fans; not considering the added mass force and damping force due to the motion of the air cushion; and considering the distribution of cushion pressure in fore and rear cushion to be uniform.

Craft dimension and coordinate system

As in sections 8.2 and 8.3, the fixed coordinate system $0\xi\eta\zeta$ and body coordinate system $GXYZ$ are both used. We introduce the following dimensions in this section (see Fig. 8.19):

l_1, l_2	Length of fore and rear skirts respectively
A_{c1}, A_{c2}	Area of fore/rear air cushion, which can be written $A_{c1} = B_c l_1, A_{c2} = B_c l_2$
X_{p1}, X_{p2}	Centre of pressure of fore/rear air cushion respectively
	$X_{p1} = (X_1 + X_g)/2$
	$X_{p2} = (X_2 + X_g)/2 \quad (8.73)$

h_{ss1}, h_{ss2}	Vertical distance from the GX axis to the lower tip of fore and rear skirts
h_{s1}, h_{s2}	Vertical distance from the GX axis to the lower tip of bow and stern skirts
h_{sg}	Vertical distance from the base plane to the lower tip of the transverse stability skirt
p_{c1}, p_{c2}	Cushion pressure of fore and rear cushion

Calculation of ACV dynamic trim over calm water

Craft trim including static hovering air gap, trim angle, etc., can be obtained by the equilibrium of forces, fan air duct characteristic and the air flow continuity equation detailed from Chapter 5. The difference of this paragraph from Chapter 5 is that for

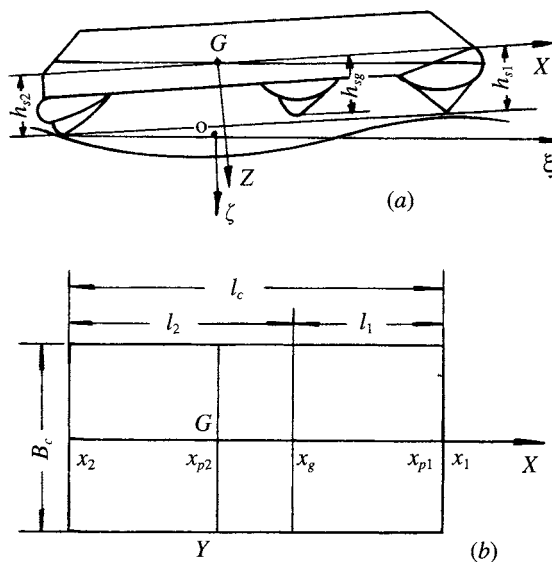


Fig. 8.19 Geometric dimensions and co-ordinate system of ACV.

the purposes of determining dynamic response, the effect of water deformation induced by wave-making on the trim is neglected for simplification of the equations. It may be noted that the SES trim running on calm water is also considered as the initial value in the case of solving the nonlinear differential equations of motion of an SES, as has been described in sections 8.2 and 8.3.

Static forces equilibrium

The static equilibrium equation for the vertical force and its moment with respect to the CG can be written as

$$\begin{aligned} A_{c1} p_{c1} + A_{c2} p_{c2} &= -W \\ A_{c1} p_{c1} X_{p1} + A_{c2} p_{c2} X_{p2} &= -M_0 \end{aligned} \quad (8.74)$$

where M_0 is the moment induced by the drag and thrust of the craft about its CG and W the craft weight. This equation can be expressed as a matrix and written as

$$[A_n][p_{ci}] = [W_n] \quad (8.75)$$

where $[A_n]$ is the geometric matrix for the air cushion:

$$[A_n] = \begin{bmatrix} -A_c & -A_{cl} \\ N_{y1} & N_{y2} \end{bmatrix}$$

$$N_{y1} = A_{cl} X_{p1}$$

$$N_{y2} = A_{c2} X_{p2}$$

$$\begin{aligned}[p_{ci}] &= \begin{bmatrix} p_{c1} \\ p_{c2} \end{bmatrix} \\ [W_m] &= \begin{bmatrix} -W \\ -M_0 \end{bmatrix} \quad (\text{the weight matrix})\end{aligned}$$

if

$$[A_{nl}] = [A_n]^{-1}$$

then

$$[p_{ci}] = [A_{nl}][W_m] \quad (8.76)$$

Fan air duct characteristic

The fan air duct characteristic equation can be written as

$$H_j = A_f + B_f Q - C_f Q^2 \quad (8.77)$$

where H_j is the total pressure of the fan, Q the inflow rate of the fan, and A_f , B_f , C_f the dimensional coefficients for the fan. We also assume that one fan is mounted on the ACV and supplies the pressurized air from the outlet of the fan via skirt bags and holes into the air cushion.

Then put

$$\begin{aligned}D &= (k\rho_a)/2A_{fk}^2 \\ E_1 &= \rho_a/(2C_{j1}^2 A_{j1}^2) \\ E_2 &= \rho_a/(2C_{j2}^2 A_{j2}^2)\end{aligned} \quad (8.78)$$

where A_j is the area of the bag holes (subscripts 1, 2 represent the fore and rear cushion respectively), C_j the flow rate coefficient, A_{fk} the characteristic area of the air duct and k the coefficient due to the energy loss of the air duct. Then the bag pressure, cushion pressure in the fore/rear cushion and flow rate can be written as

$$\begin{aligned}p_t &= H_j - DQ^2 \\ p_{c1} &= p_t - E_1 Q_1^2 \\ p_{c2} &= p_t - E_2 Q_2^2 \\ Q &= Q_1 + Q_2\end{aligned} \quad (8.79)$$

From equations (8.77) and (8.79) we have

$$p_t = A_f + B_f Q - (C_f + D)Q^2 \quad (8.80)$$

If p_{c1} and p_{c2} are given, then the bag pressure, flow rate Q , Q_1 , Q_2 and total pressure head of fan H_j can be obtained as the solution of these combined equations.

Flow rate continuity

The flow rate leaked from the fore/stern cushion can be written as

$$\begin{aligned}Q_1 &= Q_{e1} + Q_{i1} \\ Q_2 &= Q_{e2} - Q_{i2}\end{aligned} \quad (8.81)$$

where Q_{e1} , Q_{e2} are the flow leaking out from the fore/rear cushion and Q_{i2} the flow leaking from fore to rear cushion.

Assume h_{eb} , h_{es} represent the air gaps under the bow/stern and side skirts respectively and can be written as

$$\begin{aligned} h_{es1} &= -\zeta_g + x \psi - h_{ss1} \\ h_{eb} &= \zeta_g + x_1 \psi - h_{s1} \\ h_{es2} &= \zeta_g + x \psi - h_{ss2} \\ h_{es} &= -\zeta_g + x_2 \psi - h_{s2} \end{aligned} \quad (8.82)$$

The air leakage area under the fore cushion can be written as

$$\begin{aligned} A_{e1} &= A_{eb} + 2A_{es1} \\ A_{es1} &= \int_{x_g}^{x_1} (-\zeta_g + x \psi - h_{ss1}) dx = -l_1 \zeta_g + l_1 x_{p1} \psi - h_{ss1} l_1 \end{aligned} \quad (8.83)$$

where A_{es1} is the air leakage under the side skirt of the fore cushion and A_{eb} the air leakage under the bow skirt, $A_{eb} = B_c h_{eb}$. Air leakage area under the side skirts of rear cushion A_{es2} and air leakage area from the rear cushion A_{e2} can be written as

$$\begin{aligned} A_{e2} &= B_c h_{es} + 2A_{es2} \\ A_{es2} &= -l_2 \zeta_g + l_2 x_{p2} \psi - h_{ss2} l_2 \end{aligned}$$

The flow from the fore/rear cushion Q_{e1} , Q_{e2} can be written as

$$\begin{aligned} Q_{e1} &= \phi_e A_{e1} (2p_a/\rho_a)^{0.5} \\ Q_{e2} &= (\phi_{es} A_{es} + 2\phi_e A_{es2}) [2p_{c2}/\rho_a]^{0.5} \end{aligned} \quad (8.84)$$

where A_{es} is the air leakage area under the stern skirt, ϕ_{es} the flow rate coefficient under the stern skirt and ϕ_e the flow rate coefficient at other places.

The rate of cross flow between the fore/rear air cushion via the transverse stability skirt is

$$Q_{i2} = \phi_{eg} (2(p_{c1} - p_{c2})/\rho_a)^{0.5} \operatorname{sgn}(p_{c1} - p_{c2}) A_{eg} \quad (8.85)$$

where ϕ_{eg} is the flow rate of cross-flow (m^3/s), A_{eg} the air leakage area of the cross-flow (m^2), $A_{eg} = B_c h_{eg}$, and h_{eg} the air gap under the transverse stability skirt (m), where

$$h_{eg} = -\zeta_g + x_g \psi - h_{sg} \quad (8.86)$$

In these equations we assume the cross-flow rate from fore to rear cushion is positive.

Substitute equations (8.82)–(8.86) into equation (8.81), then

$$[Q] = [A_Q] [\zeta_\psi] + [A_h] \quad (8.87)$$

where

$$\begin{aligned} [Q_i] &= \begin{bmatrix} Q_1 \\ Q_2 \end{bmatrix} \\ [\zeta_\psi] &= \begin{bmatrix} \zeta_g \\ \psi \end{bmatrix} \end{aligned}$$

$$[A_Q] = \begin{bmatrix} A_{Q11} & A_{Q12} \\ A_{Q21} & A_{Q22} \end{bmatrix}$$

$$[A_h] = \begin{bmatrix} A_{h1} \\ A_{h2} \end{bmatrix}$$

where

$$\begin{aligned} A_{Q11} &= -\phi_e V_{e1} (2l_1 + B_c) - \phi_{eg} V_{el2} B_c \\ A_{Q12} &= \phi_e V_{e1} (B_c x_1 + l_1 x_{pl}) + \phi_{eg} V_{el2} B_c x_g \\ A_{Q21} &= -V_{e2} (\phi_{es} B_c + 2\phi_e l_2) + \phi_{eg} V_{el2} B_c \\ A_{Q22} &= V_{e2} (\phi_{es} B_c x_2 + 2\phi_e l_2 x_{pl}) - \phi_{eg} V_{el2} B_c x_g \\ A_{h1} &= -\phi_e V_{e1} (h_{s1} B_c + 2h_{ss1} l_1) - \phi_{eg} V_{el2} B_c h_{sg} \\ A_{h2} &= V_{e2} (\phi_{es} B_c + 2\phi_e h_{ss2} l_2) + \phi_{eg} V_{el2} B_c h_{sg} \end{aligned}$$

where

$$V_{e1} = (2p_{cl}/\rho_a)^{0.5}$$

$$V_{e2} = (2p_{c2}/\rho_a)^{0.5}$$

$$V_{el2} = (2(|p_{cl} - p_{c2}|)p_a/\rho_a)^{0.5} \operatorname{sgn}(p_{cl} - p_{c2})$$

From equation (8.87), put

$$[A_Q] = [AQ]^{-1} \quad \text{and} \quad [QA_h] = [Q] - [A_h]$$

Then the running attitude of the craft can be written as

$$[\zeta_y] = [AQ_1] [QA_h] \quad (8.88)$$

Wave equation

With respect to coordinates $0, \xi \eta \zeta$, the two-dimensional wave surface can be written as

$$\zeta_w = \zeta_a \sin(Kx + \omega_e t) \quad (8.47)$$

The vertical velocity of wave motion and wave slope can be expressed as

$$\dot{\zeta}_w = \zeta_a \omega_e \cos(Kx + \omega_e t) \quad (8.48)$$

If we put

$$A\zeta_w = \zeta_a \sin \omega_e t$$

and

$$A\dot{\zeta}_w = \zeta_a \omega_e \cos \omega_e t \quad (8.89)$$

then

$$\begin{bmatrix} \zeta_w \\ \dot{\zeta}_w \end{bmatrix} = \begin{bmatrix} \cos Kx & \sin Kx/\omega_e \\ -\omega_e \sin Kx & \cos Kx \end{bmatrix} \begin{bmatrix} A\zeta_w \\ A\dot{\zeta}_w \end{bmatrix} \quad (8.90)$$

Longitudinal linear differential equations of motion of ACVs in regular waves

Longitudinal linear differential equations of motion with small perturbation are

$$[W_I] \begin{bmatrix} \Delta \ddot{\zeta}_g \\ \Delta \ddot{\psi} \end{bmatrix} = [A_n] \begin{bmatrix} \Delta p_{c1} \\ \Delta p_{c2} \end{bmatrix} \quad (8.91)$$

in which the inertia matrix is

$$[W_I] = \begin{bmatrix} W/g & 0 \\ 0 & I_y \end{bmatrix}$$

where I_y is the pitch moment of inertia of the craft.

Air cushion system

Flow rate-pressure head linear equation with small perturbation

Under small perturbations the change of both cushion pressure and flow rate are small, thus the nonlinear equation due to the fan characteristic can be dealt with as a linear equation. From equation (8.80)

$$\Delta P_t = P_{tQ} (\Delta Q_1 + \Delta Q_2) \quad (8.92)$$

where

$$P_{tQ} = B_f - 2Q(C_f + D)$$

From equation (8.79), the fore/rear cushion pressure can be written in matrix form, as

$$\begin{bmatrix} \Delta p_{c1} \\ \Delta p_{c2} \end{bmatrix} = \begin{bmatrix} \Delta p_t \\ \Delta p_t \end{bmatrix} + \begin{bmatrix} -2E_1 Q_1 & 0 \\ 0 & -2E_1 Q_1 \end{bmatrix} \begin{bmatrix} \Delta Q_1 \\ \Delta Q_2 \end{bmatrix} \quad (8.93)$$

Substitute equation (8.92) into (8.93) and after straightening out, we obtain

$$\begin{bmatrix} \Delta p_{c1} \\ \Delta p_{c2} \end{bmatrix} = [p] \begin{bmatrix} \Delta Q_1 \\ \Delta Q_2 \end{bmatrix}$$

The elements of matrix $[p]$ are as follows:

$$[p] = \begin{bmatrix} p_{11} & p_{12} \\ p_{21} & p_{22} \end{bmatrix}$$

where

$$p_{11} = p_{tQ} - 2E_1 Q_1$$

$$p_{12} = p_{21} = p_{tQ}$$

and

$$p_{22} = p_{tQ} = 2E_2 Q_2$$

Considering $[P]^{-1}$ as the inverse matrix of $[P]$, then

$$[P]^{-1} = [Q_p]$$

i.e.

$$\begin{bmatrix} \Delta Q_1 \\ \Delta Q_2 \end{bmatrix} = [Q_p] \begin{bmatrix} \Delta p_{c1} \\ \Delta p_{c2} \end{bmatrix} \quad (8.94)$$

Small perturbation equation for flow rate of air leakage and cross-flow

Differentiating the variables Q_{c1} , Q_{c2} , Q_{12} in equations (8.84) and (8.85), putting the summation together and considering the effect of waves on the air leakage area, we have

$$\begin{bmatrix} \Delta Q_{c1} + \Delta Q_{12} \\ \Delta Q_{c2} + \Delta Q_{22} \end{bmatrix} = [AQ] \begin{bmatrix} \Delta \zeta_g \\ \Delta \psi \end{bmatrix} + [A_p] \begin{bmatrix} \Delta p_{c1} \\ \Delta p_{c2} \end{bmatrix} + [A_w] \begin{bmatrix} \Delta \zeta_w \\ \Delta \dot{\zeta}_w \end{bmatrix} \quad (8.95)$$

where A_Q can be obtained from equation (8.87),

$$[A_p] = \begin{bmatrix} A_{p11} & A_{p12} \\ A_{p21} & A_{p22} \end{bmatrix}$$

where the elements of the matrix can be written as

$$A_{p11} = \frac{Q_{c1}}{2p_{c1}} + \frac{Q_{12}}{2(p_{c1} - p_{c2})}$$

$$A_{p12} = -\frac{Q_{12}}{2(p_{c1} - p_{c2})}$$

$$A_{p21} = A_{p12}$$

$$A_{p22} = \frac{Q_{c2}}{2p_{c2}} + \frac{Q_{12}}{2(p_{c1} - p_{c2})}$$

The elements of matrix $[A_w]$ can be obtained by assuming the sums of flow from bow to stern and longitudinal flow due to the vertical displacement of waves are Q_{ew1} and Q_{ew2} so that

$$Q_{ew1} = Q_{ewb} + Q_{ews1} + Q_{ew12}$$

$$Q_{ew2} = Q_{ews} + Q_{ews2} + Q_{ew12}$$

where Q_{ewb} , Q_{ews} are the flow rate under the bow/stern skirts due to the waves, Q_{ews1} , Q_{ews2} the flow rate under the side skirts of fore/rear cushion due to the waves and Q_{ew12} the longitudinal flow due to the waves. Then

$$\begin{aligned} Q_{ew1} &= \phi_e V_{e1} \left[B_c \zeta_a \sin(Kx_1 + \omega_e t) + 2 \int_{x_g}^{x_1} \zeta_a \sin(Kx + \omega_e t) dx \right] \\ &\quad + \phi_{eg} V_{e12} B_c \zeta_a \sin(Kx_g + \omega_e t) \\ Q_{ew2} &= \phi_e V_{e2} \left[B_c \zeta_a \sin(Kx_2 + \omega_e t) + 2\phi_e V_{e2} \int_{x_g}^{x_1} \zeta_a \sin(Kx + \omega_e t) dx \right] \\ &\quad + \phi_{eg} V_{e12} B_c \zeta_a \sin(Kx_g + \omega_e t) \end{aligned}$$

If we integrate this equation and put $C_{w1} = \pi l_1/L_w$ and $C_{w2} = \pi l_2/L_w$, then

$$\begin{bmatrix} Q_{ew1} \\ Q_{ew2} \end{bmatrix} = [A_w] \begin{bmatrix} \Delta \zeta_w \\ \Delta \dot{\zeta}_w \end{bmatrix} \quad (8.96)$$

$$A_{w11} = \phi_e V_{e1} B_c \cos(Kx_1) + 2\phi_e V_{e1} l_1 [\sin C_{w1}/\sin C_{w2}] (\cos Kx_{p1}) \\ + \phi_{eg} V_{e12} B_c \cos(Kx_g)$$

$$A_{w12} = \phi_e V_{e1} B_c [\sin(Kx_1)]/\omega_e + 2\phi_e V_{e1} l_1 \sin C_{w1}/C_{w1} + [\sin(Kx_{p1})]/\omega_e \\ + \phi_{eg} V_{e12} B_c [\sin(Kx_g)]/\omega_e$$

$$A_{w21} = \phi_{es} V_{e2} B_c \cos(Kx_2) + 2\phi_e V_{e2} l_2 [\sin C_{w2}/C_{w2}] (\cos Kx_{p2}) \\ - \phi_{eg} V_{e12} B_c \cos(Kx_g)$$

$$A_{w22} = \phi_e V_{e2} B_c [\sin(Kx_2)]/\omega_e + 2\phi_e V_{e2} l_2 [\sin C_{w2}/C_{w2}] (\sin(Kx_{p2}))/\omega_e \\ + \phi_{eg} V_{e12} B_c [\sin(Kx_g)]/\omega_e$$

Flow continuity equation for small perturbations

In previous paragraphs we have developed the linear equations for change of flow rate. In this section we will use these to derive expressions for the change of flow rate due to the wave pumping, motion pumping and compressibility of the cushion air, which can be expressed as

$$\begin{bmatrix} \Delta Q_1 \\ \Delta Q_2 \end{bmatrix} = \left(\frac{\Delta Q_{e1} + \Delta Q_{12}}{\Delta Q_{e2} - \Delta Q_{12}} \right) + \frac{\Delta Q_{e1}}{\Delta Q_{e2}} \quad (8.97)$$

where ΔQ_{e1} , ΔQ_{e2} represent the total change of flow rate due to the wave pumping, motion pumping and the density change of cushion air induced by its compressibility and which can be expressed as

$$\Delta Q_{e1} = 1/\rho_a \frac{d}{dt} (\rho_a V_{c1}) = \Delta \dot{V}_{c1} + \frac{V_{c1}}{\rho_a} \dot{\rho}_a$$

$$\Delta Q_{e2} = 1/\rho_a \frac{d}{dt} (\rho_a V_{c2}) = \Delta \dot{V}_{c2} + \frac{V_{c2}}{\rho_a} \dot{\rho}_a$$

Therefore

$$\begin{bmatrix} \Delta Q_{e1} \\ \Delta Q_{e2} \end{bmatrix} = \begin{bmatrix} \Delta \dot{V}_{c1} \\ \Delta \dot{V}_{c2} \end{bmatrix} + [Q_{pd0}] \begin{bmatrix} \Delta \dot{p}_{c1} \\ \Delta \dot{p}_{c2} \end{bmatrix} \quad (8.98)$$

The first right-hand term of this equation represents the flow rate due to the wave pumping and motion pumping of the craft and the second term represents the flow due to the compressibility of the cushion air. The same as in sections 8.2 and 8.3, this flow rate can be expressed as (cf. equations 8.61 and 8.62)

$$\Delta \dot{V}_{c1} = \int_{x_g}^{x_1} [-\dot{\zeta}_g + x \Delta \dot{\psi} + \zeta_a \omega_e \cos(Kx + \omega_e t)] B_c dx$$

If we integrate this expression, then

$$\Delta \dot{V}_{c1} = (-\dot{\zeta}_g + x_p \Delta \dot{\psi}) A_{cl} + \sin C_{w1}/C_{w1} A_{cl} \omega_e \zeta_a \cos(Kx_{p1} + \omega_e t)$$

and similarly

$$\Delta \dot{V}_{c2} = (-\dot{\zeta}_g + x_{p2} \Delta \dot{\psi}) A_{c2} + \sin C_{w2}/C_{w2} A_{c2} \omega_e \zeta_a \cos (Kx_{p2} + \omega_e t)$$

Thus the sum of flow rates due to the wave pumping in fore/rear cushions can be expressed in matrix form as

$$\begin{bmatrix} \Delta \dot{V}_{c1} \\ \Delta \dot{V}_{c2} \end{bmatrix} = [Q_{zD}] \begin{bmatrix} \Delta \zeta_g \\ \Delta \dot{\psi} \end{bmatrix} + [V_w] \begin{bmatrix} \Delta \zeta_w \\ \Delta \dot{\zeta}_w \end{bmatrix} \quad (8.99)$$

where $[Q_{zD}]$ represents the motion pumping matrix, in which the various elements are

$$\begin{aligned} Q_{zD11} &= -A_{e1} & Q_{zD12} &= A_{e1} x_{p1} \\ Q_{zD21} &= -A_{e2} & Q_{zD22} &= A_{e2} x_{p2} \end{aligned} \quad (8.100)$$

$[V_w]$ represents the wave pumping matrix, in which the elements are

$$\begin{aligned} V_{w11} &= -(\sin C_{w1})/C_{w1} A_{e1} \omega_e \sin (Kx_{p1}) \\ V_{w12} &= (\sin C_{w1})/C_{w1} A_{e1} \cos (Kx_{p1}) \\ V_{w21} &= -(\sin C_{w2})/C_{w2} A_{e2} \omega_e \sin (Kx_{p2}) \\ V_{w22} &= (\sin C_{w2})/C_{w2} A_{e2} \cos (Kx_{p2}) \end{aligned}$$

We assume the change of air cushion complies with the adiabatic principle, therefore its matrix expression is

$$[Q_{pD0}] = \begin{bmatrix} V_{c1}/(1.4(p_a + p_{c1})) & 0 \\ 0 & V_{c2}/(1.4(p_a + p_{c2})) \end{bmatrix}$$

Now we can substitute the matrix of flow rate into the air cushion (8.94), the matrix of flow rate due to air leakage from the cushion, the wave pumping, motion pumping and matrix representing the flow rate due to the compressibility of cushion air (8.98) into the matrix representing the flow rate continuity equation (8.97) and after straightening out, then

$$[Q_{pc}] \begin{bmatrix} \Delta p_{c1} \\ \Delta p_{c2} \end{bmatrix} + [Q_{pD}] \begin{bmatrix} \Delta \dot{p}_{c11} \\ \Delta \dot{p}_{c21} \end{bmatrix} = [A_Q] \begin{bmatrix} \Delta \zeta_g \\ \Delta \psi \end{bmatrix} + [Q_{zD}] \begin{bmatrix} \Delta \dot{\zeta}_g \\ \Delta \dot{\psi} \end{bmatrix} + [Q_{zw}] \begin{bmatrix} \Delta \zeta_w \\ \Delta \dot{\zeta}_w \end{bmatrix}$$

where

$$[Q_{pc}] = [Q_p] - [A_p]$$

$$[Q_{pD}] = -[Q_{pD0}]$$

$$[Q_{zw}] = [A_w] + [V_w]$$

Put $[p_{cQ}] = [Q_{pc}]^{-1}$ and multiply the left/right terms of equation (8.100) by $[p_{cQ}]$, then

$$\begin{bmatrix} \Delta p_{c1} \\ \Delta p_{c2} \end{bmatrix} + [T_c] \begin{bmatrix} \Delta \dot{p}_{c1} \\ \Delta \dot{p}_{c2} \end{bmatrix} = [p_{zc}] \begin{bmatrix} \Delta \zeta_g \\ \Delta \psi \end{bmatrix} + [p_{zD}] \begin{bmatrix} \Delta \dot{\zeta}_g \\ \Delta \dot{\psi} \end{bmatrix} + [p_w] \begin{bmatrix} \Delta \zeta_w \\ \Delta \dot{\zeta}_w \end{bmatrix} \quad (8.101)$$

where

$$[T_c] = [p_{cQ}] [Q_{pD}]$$

$$[p_{zc}] = [p_{cQ}] [A_Q]$$

$$[p_{zD}] = [p_{cQ}] [Q_{zD}]$$

$$[p_w] = [p_{cQ}] [Q_{zw}]$$

Put equation (8.101) in Laplace transformation, then

$$\{[T_c]S + [I]\} \begin{bmatrix} \Delta p_{c1}(S) \\ \Delta p_{c2}(S) \end{bmatrix} = \{[p_{zD}]S + [p_{zc}]\} \begin{bmatrix} \Delta \zeta_g(S) \\ \Delta \psi(S) \end{bmatrix} + \{[p_{wD}]S + [p_{wc}]\} \Delta \zeta_w(S) \quad (8.102)$$

where $[I]$ is the unit matrix and S the Laplace operator.

Solution of the linear differential equations of motion

Applying Laplace transformation to the linear differential equations of motion (8.91) and substituting into expression (8.102), the motion equations can be expressed as

$$[A(S)] \begin{bmatrix} \Delta \zeta_g(S) \\ \Delta \psi(S) \end{bmatrix} = [B(S)] \Delta \zeta_w(S) \quad (8.103)$$

where $[A(S)]$ is the matrix representing the characteristic coefficients for the craft, which can be written as

$$[A(S)] = [A_0]S^3 + [A_1]S^2 + [A_2]S + [A_3] \quad (8.104)$$

where

$$[A_0] = [A_n] [T_c] [A_{n1}] [W_I]$$

$$[A_1] = [W_I]$$

$$[A_2] = -[A_n] [p_{zD}]$$

$$[A_3] = -[A_n] [p_{zc}]$$

$[B(S)]$ is the matrix representing the coefficient of wave perturbation force and can be written as

$$[B(S)] = [B_0]S + [B_1] \quad (8.105)$$

where

$$[B_0] = [A_n] [p_{wD}]$$

$$[B_1] = [A_n] [p_{wc}]$$

From equation (8.103), the transfer matrix of motion can be written

$$[D \zeta_g(S)] = [A(S)]^{-1} [B(S)] \quad (8.106)$$

Substitute $S = j\omega_e$ into the foregoing matrix, then the frequency response characteristics for craft motion and wave perturbation force can be obtained.

So far, we have introduced the formation of the linear differential equations of motion of ACVs in regular waves. Although the deformation of the wave surface induced by the air cushion and the hydrodynamic force acting on the skirts have not been taken into account, the equations are expressed in matrix form and use the Laplace transformation to obtain the simplified equation, which is similar to that for conventional ships and is easy to solve and analyse.

However, it may be noted that there are some differences between the theoretical method and the practical situation, particularly for modern coastal ACV/SES with responsive skirts. This will lead to some prediction errors.

Calculation results and analysis

Reference 69 described the calculation of longitudinal motion response of an ACV of 5, 20, 60, 200 and 400 t to regular waves and predicted the seaworthiness qualities of an ACV in sea state 3 in the East China Sea with the aid of spectral analysis in order to analyse its seaworthiness and the effect of compressibility of cushion air. The main parameters used were:

Froude number	Fr	= 1.6
Cushion length-beam ratio	l_c/B_c	= 2
Non-dimensional mass coefficient of craft	$Wl(\rho_w g l_c^3)$	= 6.6×10^{-3}
Non-dimensional inertia coefficient of craft	$I_y/(\rho_w g l_c^5)$	= 5.2×10^{-4}
Non-dimensional length of skirt	h_s/l_c	= 0.078
Non-dimensional horizontal location of transverse stability skirt	X_g/l_c	= 0.023
Non-dimensional area of skirt holes in fore air cushion	A_{j1}/l_c^2	= 0.0136
Non-dimensional area of skirt holes in fore air cushion	A_{j2}/l_c^2	= 0.0111

The analysis and comparison between the calculation and experimental results can be summarized as follows:

Heave response

The frequency responses of heave amplitude for the ACVs weighing 5t(A) and 400 t(B) in waves are shown in Fig. 8.20. The trend of the curves is similar to that for an SES, in which an amplitude peak exists at low frequency ($\omega_e [l_c/g]^{0.5} \approx 5$), which is induced by the coupled pitch-heave motion. Figure 8.21 shows the frequency response of pitch amplitude for the ACVs in waves.

In the case where the pitch motion response is smooth, a small step of amplitude will appear here, otherwise there will be a peak and the relative amplitude will be greater

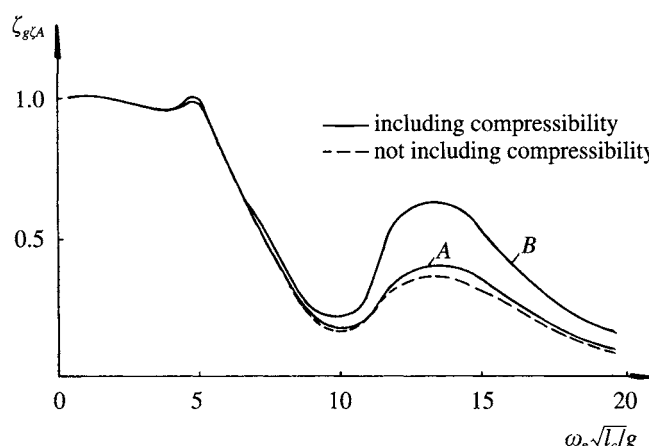


Fig. 8.20 Unit frequency response of heave amplitude for ACV in waves. A: 5 t craft, B: 400 t craft.

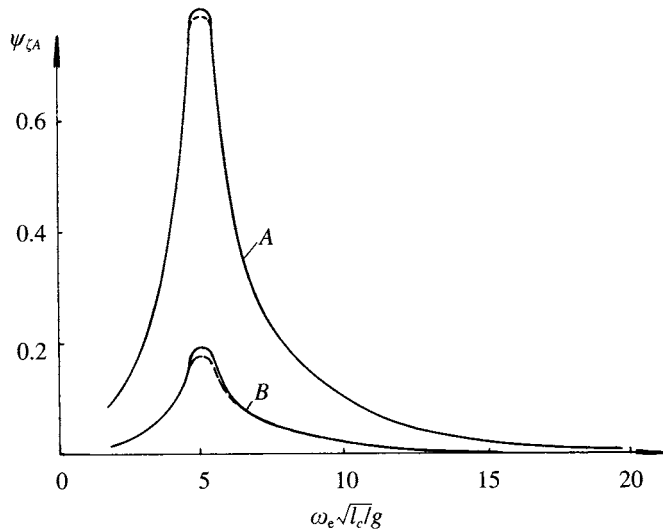


Fig. 8.21 Unit frequency response of pitch amplitude for ACV in waves (see Fig. 8.20 for key).

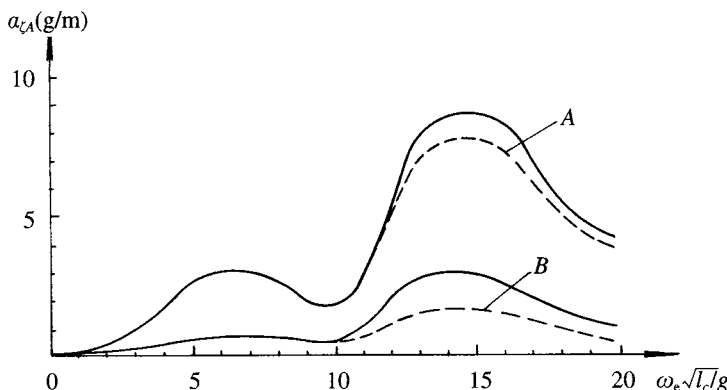


Fig. 8.22 Unit frequency response of heave acceleration for ACV in waves (see Fig. 8.20 for key).

than 1. The formation of a peak amplitude of heave at high frequency, and a hollow at medium frequency is closely related to the wave perturbation force as shown in Fig. 8.23.

When the relative period length ratio $\omega_e [l_c/g]^{0.5} \approx 10$ and $L_w (1.25 \sim 1.5)l_c$, the wave-pumping effect and wave perturbation force will be so small as to form the hollow on the curve of the wave perturbation force. But when the relative period length ratio $\omega_e [l_c/g]^{0.5} \approx 14$ and $L_w \approx 0.9l_c$, then the wave perturbation force will be so large as to form the peak on the curve of wave perturbation, at which the heave natural frequency is situated.

Pitch response

Figure 8.21 shows the curve of frequency response of pitch motion; it can be seen that the steep amplitude peak is situated at $\omega_e [l_c/g]^{0.5} \approx 5$, namely at the pitch natural

frequency. The figure shows the characteristics of a system with low damping, low stability and low natural frequency of pitch motion. The peak disturbance moment occurs at $\omega_e [l_c/g]^{0.5} \approx 8 \sim 10$, where the wavelength $L_w \approx 1.5l_c$ (see Fig. 8.24). Sometimes a small peak also exists at this relative frequency.

Vertical accelerations

Figure 8.22 shows the frequency response of vertical accelerations, in which the peak vertical acceleration is estimated to be induced by pitch motion, but peak vertical acceleration at high frequency is caused by heave motion. Thus it can be seen that the vertical acceleration at the bow will be reduced considerably if the pitch motion damping rate can be increased and the quasi-static stability in heave motion can be decreased.

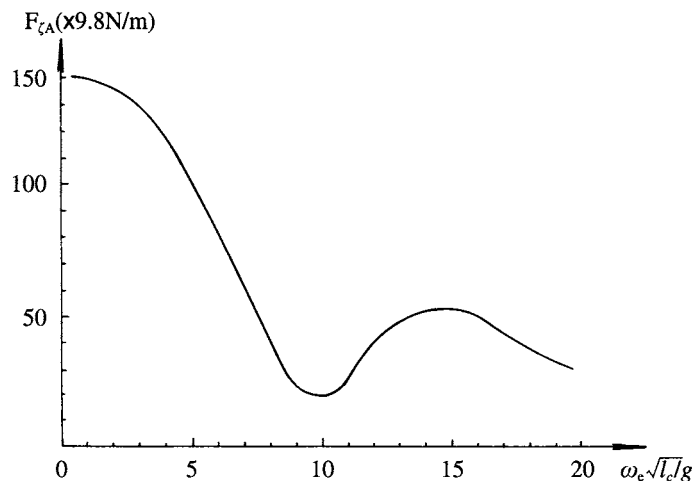


Fig. 8.23 Unit frequency response for wave exciting force.

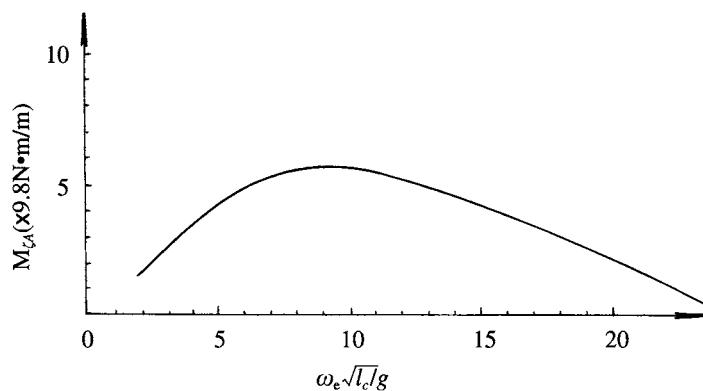


Fig. 8.24 Unit frequency response for wave exciting moment.

Compressibility

All the figures mentioned above from Fig. 8.20 to 8.26 include the effect of compressibility on the motion, thus it can be seen that the effect of compressibility increases with the all-up weight of the craft. Figure 8.25 shows that if K_p represents the percentage increase of significant bow vertical acceleration due to the effect of cushion air compressibility, then it can be seen that $K_p = 2.5\%$ for the craft of 5 t ($I_c \approx 10$), i.e. the effect of compressibility of cushion air can be neglected, but $K_p = 41\%$ for the craft of 400 t, which means that in this case the cushion air compressibility cannot be neglected.

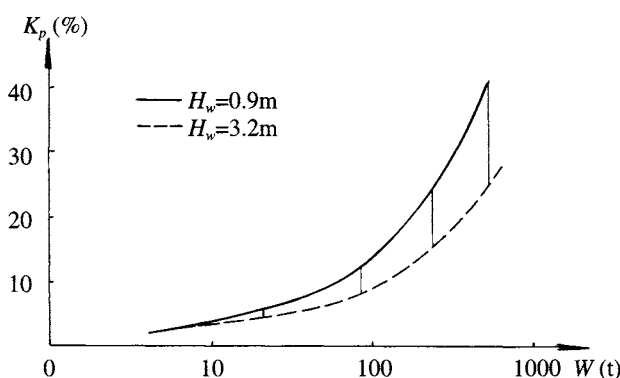


Fig. 8.25 Influence of cushion air compressibility on ACV seaworthiness.

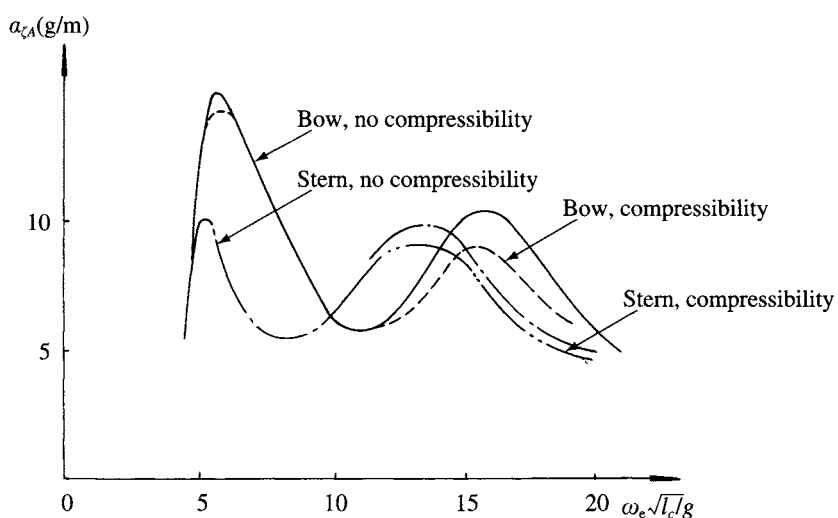


Fig. 8.26 Unit frequency response for acceleration at bow/stern.

We have now introduced the coupled motion for both longitudinal/transverse directions of ACV/SES in waves. Strictly speaking, the calculations are not perfect for the following reasons:

1. Response of the skirt to the waves has not been considered.
2. Wave surface deformation due to the air cushion pressure pattern has not been taken into account.
3. The calculations do not take the dynamic response of the fans into account, where ACV/SES are heaving and pitching while moving through the waves, particularly in the case of high craft speed.
4. The damping coefficient and added mass due to wave-making caused by the motion of the hovercraft, and the interference between the air cushion and side-walls are also not taken into account.

All of these problems should be eased in further research work in the future.

8.5 Motion of ACV and SES in short-crested waves

Both ACVs and SESs will be excited at high frequency when they are running over short-crested waves (or three-dimensional waves), just like an automobile running on a road surface with a lot of cobblestones. Thus this physical phenomenon is called the ‘cobblestone effect’ and which upsets the crew and passengers. The Chinese SES 7203 had such an experience when the craft was on the Wang Puan river, but the phenomenon disappeared when the craft left the river and entered the mouth of the Yangtze, a wider and deeper waterway. Because the motion response is an ultra-short one, such a phenomenon is therefore very difficult to describe by theoretical methods.

Of course this phenomenon can be simulated in a towing tank for qualitative analysis, but the theoretical basis for it is not yet fully understood. The rationale, cause and solution of the cobblestoning effect are not clear, therefore we are obliged to analyse this physical phenomenon qualitatively, as below.

Compressibility effect of air cushion air

When the ACV/SES are running in short-crested waves, the compressibility effect will be considerable although the waves are not high. Only the SES version 7203 of all of the ACV/SES designed by MARIC is strongly sensitive to the cobblestoning effect with large vertical acceleration. In our experience, this is expressed by the slamming or the higher upward vertical acceleration; and it is rather different with the craft running in long waves, in which the craft will be accelerated downward, i.e. the crews or equipment will suffer from a sense of loss in weight.

This effect will probably be due to the sudden increase of cushion pressure. From Fig. 8.20, it is found that a peak vertical acceleration is located at high encounter frequency with the influence of compressibility. Figure 8.20 shows the operation of the ACV running in regular waves compared with the craft running in the three diagonal waves, the instantaneous flow rate of the craft is probably equal to zero ($Q_e = 0$); in this case, the effect of air cushion compressibility will be enhanced. In order to simplify the estimation, we assume the change of air condition in the cushion complies with Boyle's law, i.e. $PV = \text{constant}$, in which P represents the cushion air pressure and V the cushion volume.

In the case where the cushion volume reduces by 10% because of the craft's

heave motion, without any outflow of air, then $p = p_a + p_c = 103\,300 + p_c$ (N/m²), in which p_a represents the atmospheric pressure and $p_c = 3000$ N/m², then the relative cushion pressure will be increased to five times the initial pressure. Of course, this is an extreme condition for estimation, but it can be demonstrated that the large heave motion in the case of a sealed air cushion will induce a large vertical acceleration.

Effect of slope of fan air duct characteristic

Although the characteristic curve of the Chinese fan model 4.73 is quite flat, the combined characteristic curve will be steep in the case where the air duct inlet or outlet is narrow, causing an increase in the flow damping coefficient.

The interference of waves

The interference of waves to the bow and stern seals will not only influence the change of air leakage area, but will also build up the response of skirts to waves because of the change of bag-cushion pressure ratio. Sometimes it will cause the sealing action of air leakage and thus present the effect mentioned in the paragraph on compressibility.

In order to improve the vertical acceleration due to the cobblestoning effect, the following measures may be adopted.

A number of measures may be taken to improve ACV ride, as follows.

Decrease of the effect of cushion air compressibility as little as possible

For instance, the delta area for air leakage between the fingers should be preserved in order to reduce the sealing effect of air leakage under the action of the waves.

Careful skirt geometry design

The bow/stern skirts have to be designed with a suitable ‘yieldability’ – particularly to avoid bounce or sealing effect. Of course this problem has still not been understood perfectly, but the balanced stern seal of SES version 713 had good results, because the cobblestoning effect was seldom encountered.

Use of the damping effect of cushion depth

High sidewalls, thus the deep cushion and large volume of the air cushion will reduce the cobblestoning effect dramatically. For instance, the sidewall depth of SES version 719G is double that on SES version 7203. Probably this is one of main reasons for no cobblestoning effect having been found on the craft version 719.

Use of flat lift fan and duct system characteristics

The fan air duct characteristic curves have to be as flat as possible, for instance, the air ducts of air inlet/outlet should be as large as possible to reduce the inflow and outflow velocity, which had not been possible to satisfy on SES version 7203. In addition, the parallel operation of multiple fans can also flatten the fan characteristic, e.g. there are two double inlet fans operating in parallel on SES version 719G and 713 but only a single inlet fan on SES version 7203, which is more sensitive to the cobblestone effect.

Figure 8.27 shows the time history for vertical acceleration of a certain SES running on three-dimensional waves at a speed of 28 knots. The wave height is rather small, only 0.2–0.3 m (1/10 highest waves) and the measured encounter frequency is about 2 Hz, vertical acceleration reaches up to 0.3 g. Perhaps this is a typical result of the cobblestoning effect.

The higher acceleration in long periods of operation causes discomfort for crew and passengers. For this reason the cobblestoning effect has to be considered seriously in ACV/SES design.

8.6 Plough-in of SES in following waves

Sometimes the plough-in phenomenon also occurs to an SES. It does not normally happen in the case of following winds as for an ACV, but it does occur in the case of following waves, particularly at the early stage of development of SES. For instance this phenomenon used to occur with the experimental SES version 711-III (weighing 2 t) of MARIC, in the case of following waves with significant wave height $h_{1/3} = 0.45$ m, i.e. $h_{1/3}/W^{0.33} > 0.3$, where W is the displacement of the craft (m^3).

Sometimes, the plough-in phenomenon even happened to craft running over stern waves induced by large tugs, while overtaking them. Figure 8.28 shows a damaged lift fan caused by plough-in of the craft; furthermore one can find that the forward guide blades are also damaged. In addition, plough-in also happened to the passenger SES version 713 in following waves with $h_{1/10} = 0.8\text{--}1.0$ m, i.e. $h_{1/10}/W^{0.33} = 0.26\text{--}0.33$. It also happened to an SES model in the towing tank of the China Ship Scientific Research Centre (CSSRC) during the seaworthiness experiments in following (regular) waves with $h/W^{0.33} = 0.22$ as shown in Fig. 8.29. Similarly, plough-in has happened to the SES version 717C when running over a ship's stern waves in cases where the cushion air supply to the bow bag was insufficient.

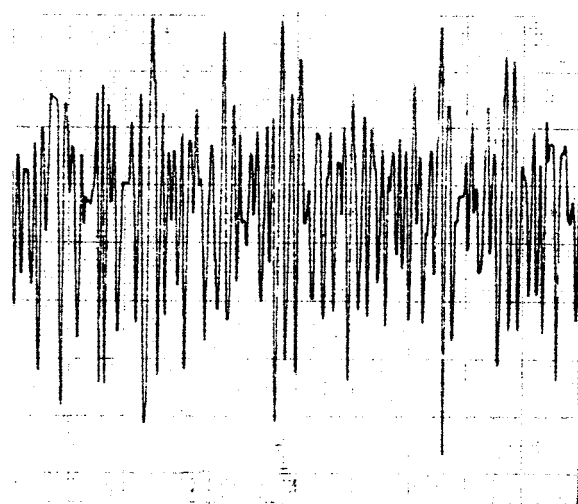


Fig. 8.27 Time history of cushion pressure fluctuation due to the 'cobblestoning effect' measured on an SES running in light waves.

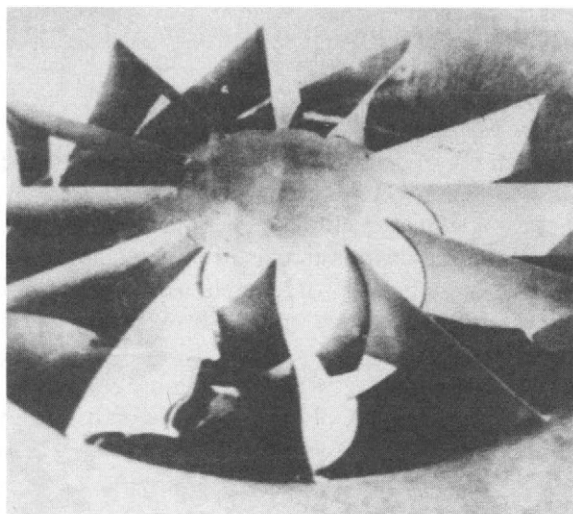


Fig. 8.28 The broken wooden fan caused by plough-in of an SES in following seas.

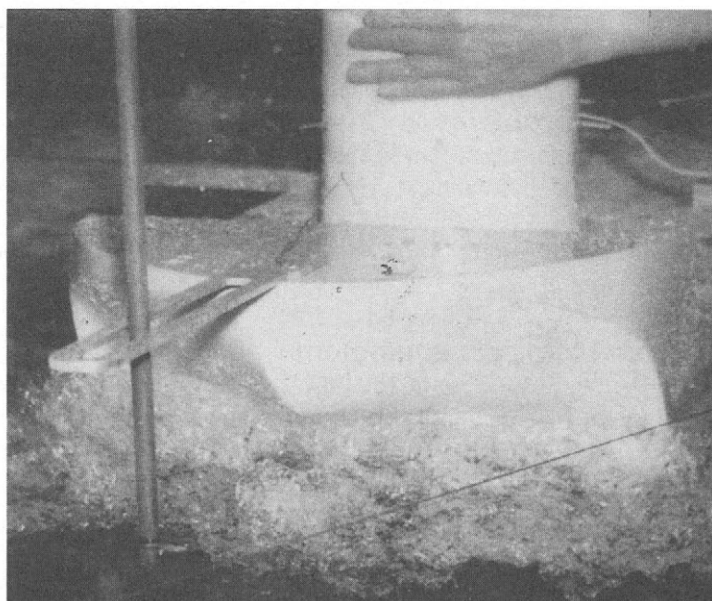


Fig. 8.29 'Plough-in' phenomenon of a SES model simulated in a towing tank.

To sum up, with respect to the SES, the plough-in phenomenon when running in following waves is very important and we will therefore present some analysis in the following subsection as a guide to the reader.

Internal reasons for plough-in

Skirt tuck-in at bow skirt

In the same way as on an ACV, tuck-under of the SES bow skirt has to be prevented. Originally, when the flexure is inward to the bow skirts, the craft will experience a bow-up moment because of increasing the bow cushion area as long as the cushion pressure can be kept constant. But actually the oncoming water flow will stick to the bow skirt to build up the internal vortices and disturb the cushion air, which will cause a drop in cushion pressure and a bow-down moment as shown in Table 8.1. The bow skirt with the long fingers, which are fitted on the SES version 711-III, is sensitive to tuck-under and has a poor pitching stability.

From Table 8.1, it is found that the craft was pitching bow down when the bow cushion pressure was dropping, causing plough-in of the craft. It may be noted that the skirt with long fingers is poor at preventing plough-in.

Lift system insufficiency

The craft lift system has to provide enough heave stability and restoring force (moment). Now in most craft of Chinese construction the industrial fan model 4-73 is fitted, with $H_{j\max}/H_{jd} \approx 1.2$ where $H_{j\max}$, represents the maximum total head at $Q = 0$ and H_{jd} the designed total pressure of the fan. In the case where Q_e increases, the restoring force due to the lift system decreases.

Lift system ducting problems

When the outlets of lift fans are mounted vertically, such as the arrangement of lift fans on passenger SES model 713 and experimental SES model 711-III, in cases where the craft was dropping down, then the water spray would be raised to impact the fans leading to a decrease in the revolution of the fans, subsequently causing the craft to plough-in.

Matching of bow/stern seal equipment

In the case where the heave stiffness of the bow and stern seal equipment does not match closely that of the bow seal and is softer at the bow, then the craft may present

Table 8.1 The test results of cushion pressure of SES version 711-III during craft plough-in

Running attitude	Cushion pressure (Nm^2)				Remarks
	Bow	Front cushion	Rear cushion	Stern	
From take-off course to post-hump speed of 40 kph	1500	1500	1400	1400	Cushion pressure steady, trim approx. $+5^\circ$
Running through a ship's stern wave	1400	2000	1600	1800	Trim approx. $+4.5^\circ$
Another take-off course	1400	1500	1600	1600	Trim approx. $+6.5^\circ$
During operation of the craft, some people were asked to move from amidships to the bow so as to cause bow-down trim	0-1500	0-2500	1300	1600	Trim approx. -4° (plough-in occurred)

a bow-down pitching moment while it is heaving down. Therefore as the balanced type stern seal matched with the long finger-type bow seal, similar to the bow/stern seal arrangement on the SES versions 71-III and 713, then the plough-in phenomenon often occurred on these craft because the heave stiffness of the stern seal was much larger than that of the bow seal.

External response

In the case where the SES is running in following waves, then the wave encounter period will increase considerably. For example, if the SES model 713 is running at speed of 30 km/h in following waves with wavelength of $L_w = 20$ to 25 m, then the wave encounter period $T_e = 10$ s, but $T_e = 2$ s in head seas. Therefore the craft has enough time to leak air in the case of running in following waves, and thus build up to plough-in.

This phenomenon can be explained practically. In the case where the SES is running in following waves, the air was initially leaked under the stern seal and rear sidewalls, then the air leakage or spray gradually moved forward. The time for air leakage at a fixed location will lengthen as the wave encounter period elongates, especially when the craft speed is close to wave velocity. Thus plough-in would occur as the location of air leakage was moving to the bow. This is why the plough-in phenomenon has occurred to SESs running in following waves, but never happened to SES in head seas.

Methods for preventing plough-in

Stiffen geometry of bow skirt area relative to stern

The bow skirt of the bag and finger type, higher bag-cushion pressure ratio and D-type bag are suggested to be mounted on SES, which can prevent tuck-under of the skirt due to the high tension on the fabrics of the bow skirt. The resistance to plough-in of SES type 717 improved considerably once this type of skirt had been mounted on the craft.

Increase fan curve gradient

Increasing the steepness of the fan air duct characteristic curve would be in conflict with the need to prevent cobblestoning, so perhaps using a winding outlet of fans is a better measure for preventing the water spray from impacting directly on the fan blades.

Adjust bow finger tip line

It suggests mounting the bow fingers flatter with respect to the base-line of the craft, which can not only reduce the water drag of the fingers, but also increase the restoring moment of pitching.

Use anti-plough-in hydrofoils

Anti-plough-in hydrofoils may be mounted at the bow as shown in Fig. 1.32, which was mounted on the experimental SES model 711-III.

Adjust relative stiffness of bow and stern skirts

The heave stiffness for bow/stern seals has to be suitably selected. In general, the heave stiffness for the bow should be greater than that for the stern seal in order to present a bow-up restoring moment in the case of heaving down, which can be obtained by means of adjusting the bag–cushion pressure ratio and responsiveness of the bow and stern bag.

Adjust air supply to bow skirt area

The air supply to the bow skirt has to be carefully taken into account. In the case where a separate bow lift fan is adopted, then the heave stiffness of the bow area can be adjusted to keep a constant bag pressure to prevent tuck-under of the bow skirt and plough-in of the skirt in following seas. In general it is advised to feed the majority of cushion air flow through the bow skirt area.

8.7 Factors affecting the seaworthiness of ACV/SES

In this section we will discuss the various factors affecting the seaworthiness of ACV/SES with a view to improving performance. Similarly as with conventional ships, the problems concerning the seaworthiness of craft to which we pay particular attention are as follows:

1. the motion amplitude and acceleration of craft running in waves, such as ζ_g , $\ddot{\zeta}_g$, ψ , $\dot{\psi}$, θ , $\dot{\theta}$, etc. and the superposition of coupled motion, which presents a combined vertical motion amplitude and acceleration, transverse and longitudinal motion amplitude and acceleration;
2. speed degradation of craft in waves;
3. the ability for taking off and maintaining high speed cushion-borne operation of craft;
4. the problems concerning the manœuvrability and stability of craft in waves;
5. the reliability of instruments, equipment, engines and hull structure on craft operating in waves.

Some problems not only concern the theory of hovercraft, but also the design methods. These aspects will be discussed in later chapters, after Chapter 10. Some problems detailed above are the problems which are under study at present, and the references concerned with these problems are fewer, such as (3) and (4). Therefore we will discuss problems (1) and (2) above and analyse these problems approximately based on some experimental data.

Effect of skirts on seaworthiness of ACV/SES

Effect of skirt height

According to [4], the drag of ACV skirts in waves can be expressed as

$$R_{rw}/(q_w l_c S_c^{0.5} = f\{2h_w/[h_c + h_f]\} = 20 \times 10^{-5} (2h_w/[h_c + h_f])^{5/3} \quad (8.107)$$

where R_{rw} is the skirt drag in waves (N), l_c the peripheral length of air cushion (m), S_c

the cushion area (m), h_w the half-wave height (m), h_c the cushion height (m), h_f the finger height (m) and

$$q_w = 0.5 \rho_w V_s^2$$

where V_s is the craft speed (m/s) and ρ_w the water density (Ns^2/m^4). This equation can also be expressed graphically as in Fig. 8.30, which demonstrates the effect of cushion depth and finger height on the wave drag: the deeper the cushion, the smaller the wave drag.

Effect of skirt type

With respect to the ACV, inclined responsive skirts with low natural frequency obtain a clear effect for improving seaworthiness. So-called inclined skirts are those with higher bow skirt than stern skirt. Thus the high bow skirt fingers and bag could reduce the wave drag. As a matter of fact, this effect has been seen on SES and the matching of higher bow skirt with a lower stern skirt was adopted on passenger SES in 1969.

The responsive skirt can decrease its natural frequency, thus it is equivalent to mounting a damper on hovercraft, which not only improves vibration at high frequencies, such as the cobblestone effect, but also improves heave motion in long waves, which causes deformation of the skirt and reduction of the vertical motion of the hull so as to move closer to platforming operation. The vertical acceleration and skirt drag will be reduced significantly.

Figure 8.31 shows the improvements in speed degradation of the craft model SR.N4 Mk 1 of BHC running in head waves and beam wind. Thanks to mounting an improved skirt on Mk 3 craft, speed loss in rough seas was reduced by 30–40%. In the case of using the new standard skirt design, then the improvement in speed loss will be less, even though the craft model Mk 3 has higher cushion length to beam ratio and larger all-up weight than the Mk1. The speed degradation has improved due to well-designed skirts.

Thanks to the improvements in skirts and elongation of cushion length/beam ratio of the Mk 3 craft, the bow vertical acceleration of SR.N4 Mk 3 in waves with

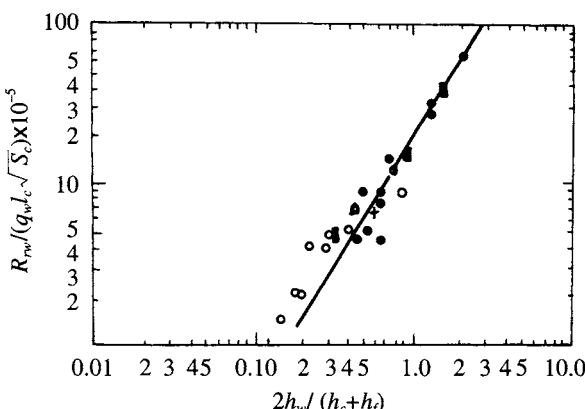


Fig. 8.30 Influence of skirt height / wave height on the skirt wave drag of ACV in waves.

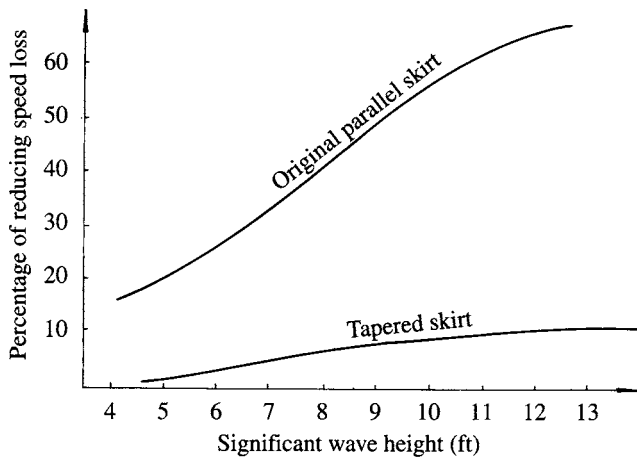


Fig. 8.31 Reduction of speed loss of SR.N4 Mk3 relative to SR.N4 Mk1 in head seas and beam winds.

significant wave height of 1.2 m reduced to 0.1 g, pitch angle (double amplitude) dropped to 1.5°, decreasing by a factor of 50% over Mk 2, vertical acceleration at the CG dropped to 0.07 g, decreasing by 25% over the Mk 2, and craft speed increased from 45 knots decreasing to 54 knots. All of these should be attributed to the success of the inclined responsive skirt with low natural frequency skirt cloth thickness.

Effect of material thickness

There are no definite conclusions on such problems, but it may be seen that a reduction of skirt cloth thickness will reduce the inertia drag of skirts, induced by flagellation of the skirt in waves. Therefore thinner skirt cloths were applied to the British military ACV model BH.7. Of course, it may influence the skirt life, particularly if the craft are often operated along sandy beaches. Since the BH.7 is a military test craft therefore the thinner skirt cloths were applied to the craft after a design trade-off.

Effect of principal dimensions on seaworthiness

Effect of l_c/b_c

The increase in l_c/b_c can always improve the seaworthiness and the speed degradation of craft both for ACVs and SES. The relation of frontal area may be one of the reasons for reducing water drag of skirts; reduction of longitudinal motion of the craft due to the increase in cushion length may be another reason for improving speed degradation.

Figure 8.32 shows a speed comparison between the SR.N4 Mk1 and Mk3 craft models. Keeping cushion pressure constant, the SR.N4 Mk1 was stretched by 16.74 m, increasing the speed in waves by 10–20% while increasing all-up weight by 44%.

Figure 8.33 shows the improvement of British SES model HM-2 by stretching of the cushion length/beam ratio from 2.45 to 2.95 and 3.58 respectively, keeping the

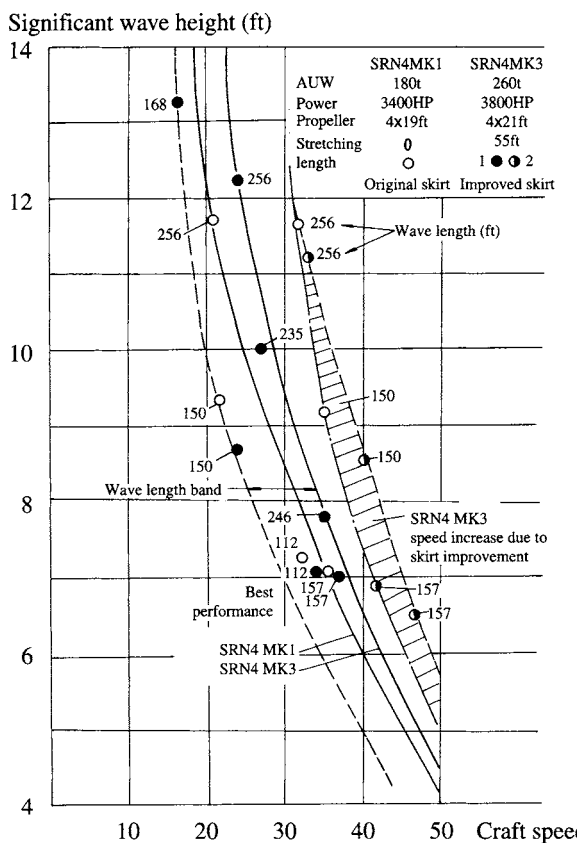


Fig. 8.32 Comparison of ship speeds between SR.N4 Mk3 and Mk1 in head seas and beam winds.

cushion pressure constant. This change was based on the original design HM.216 keeping cushion beam constant, then stretching the cushion length and thus the all-up weight of the craft, while keeping engine output approximately constant. Thus it is found that the speed degradation of the craft improves greatly in waves with significant height of 0.8–1.0 m. Meanwhile, the calm water performance, particularly at low and medium speeds, drag hump, overload capability and economy of the craft are also significantly improved.

For this reason, the stretching of ACV/SES is the modern way to improve craft performance. With the stretching of the Chinese SES craft 717 and 719, the speed performance, seaworthiness and economy of both craft were also very much improved.

Figure 8.34 demonstrates the speed degradation of various craft in waves. It is seen that the speed loss of craft with high cushion length/beam ratio is lower than those with low length/beam ratio at different ratios.

Figure 8.35 shows the comparison of pitch response factors between the craft model SR.N4 Mk 1 and SR.N4 Mk 3 in waves; thanks to the improvement of the skirt and elongation of the cushion length/beam ratio of the craft model Mk 3, the pitch attitude response decreased by 50–100%.

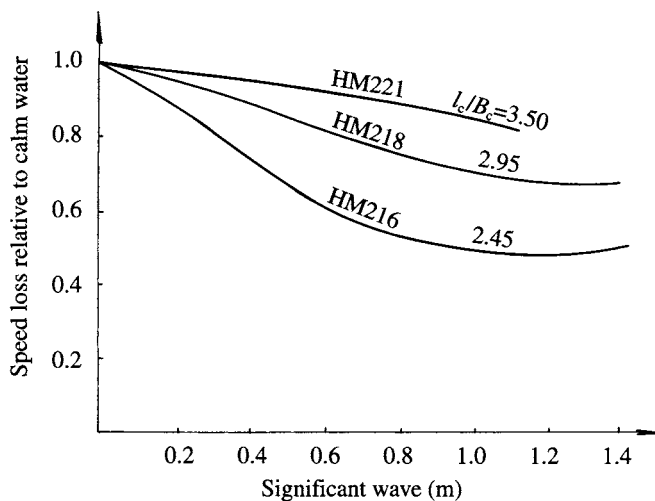


Fig. 8.33 Speed improvement of British SES in waves due to the increment of cushion length-beam ratio.

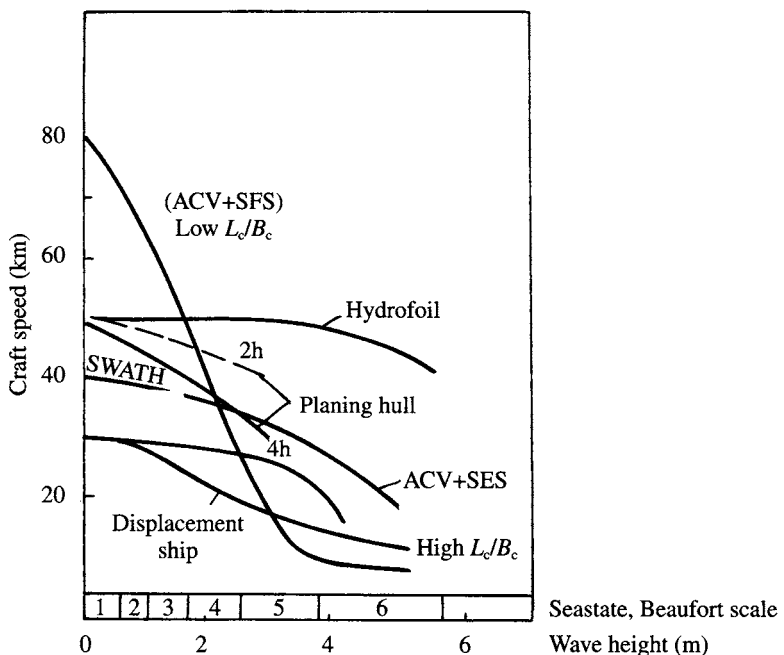


Fig. 8.34 Comparison of sustainable ship speed in different sea states between various types of ships weighing 200 t.

Effect of sidewall thickness ratio B_{sw}/B_c

An increase in the sidewall thickness ratio B_{sw}/B_c (where B_{sw} is sidewall thickness, B_c is cushion beam) will improve the seaworthiness, reduce vertical acceleration and

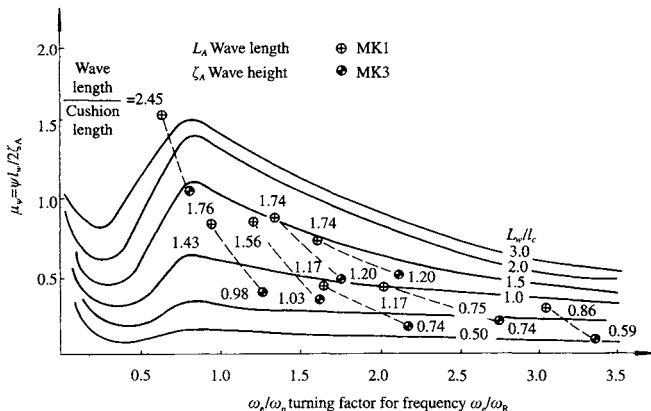


Fig. 8.35 Frequency response of pitch amplitude for SR.N4 Mk1 and SR.N4 Mk3 models in waves.

improve speed loss in waves, because the fluctuation of cushion pressure will decrease in the case of thicker sidewalls, which then reduces the heave acceleration.

One must be careful not to increase sidewall width too far, since if more than about 30% of the craft weight is taken by sidewall planing pressure on the sidewall lower surface, then motions begin to be controlled by these hydrodynamic forces rather than be supported from the cushion, and drag forces will increase greatly.

Effect of sidewall depth H_{sw}

Increased H_{sw} , thus increase in cushion depth and cushion volume, will decrease the effect due to the wave pumping, motion pumping and compressibility of the cushion air, thus will decrease the perturbation of waves on the hull motion and improve seaworthiness. Therefore sidewall depth and skirt depth will be increased in the case of craft with good seaworthiness.

Effect of inner draft of sidewall

Increase of the inner draft of the sidewall will decrease the nonlinear air leakage (Q_{esw}) in waves, so as to decrease the wave perturbation force (moment), therefore the seaworthiness will be improved in the case where the skirts can be adjusted automatically.

Effect of damping on seaworthiness

Besides the change of motion natural frequency to avoid resonance with the wave encounter frequency, the increase of motion damping may be one of the most efficient measures to decrease the motion amplitude at the resonance frequency, particularly in the case of pitch motion, because the latter has the characteristic of small damping and small stability with respect to the heave motion. Specific measures are as follows.

Pitch damping

The bow hydrofoils can be fitted at the bow of an SES to increase damping pitch, thus improving the seaworthiness efficiently. Figure 8.36 shows the effect of hydrofoils with different dimension ratio on the seaworthiness of an SES model [75].

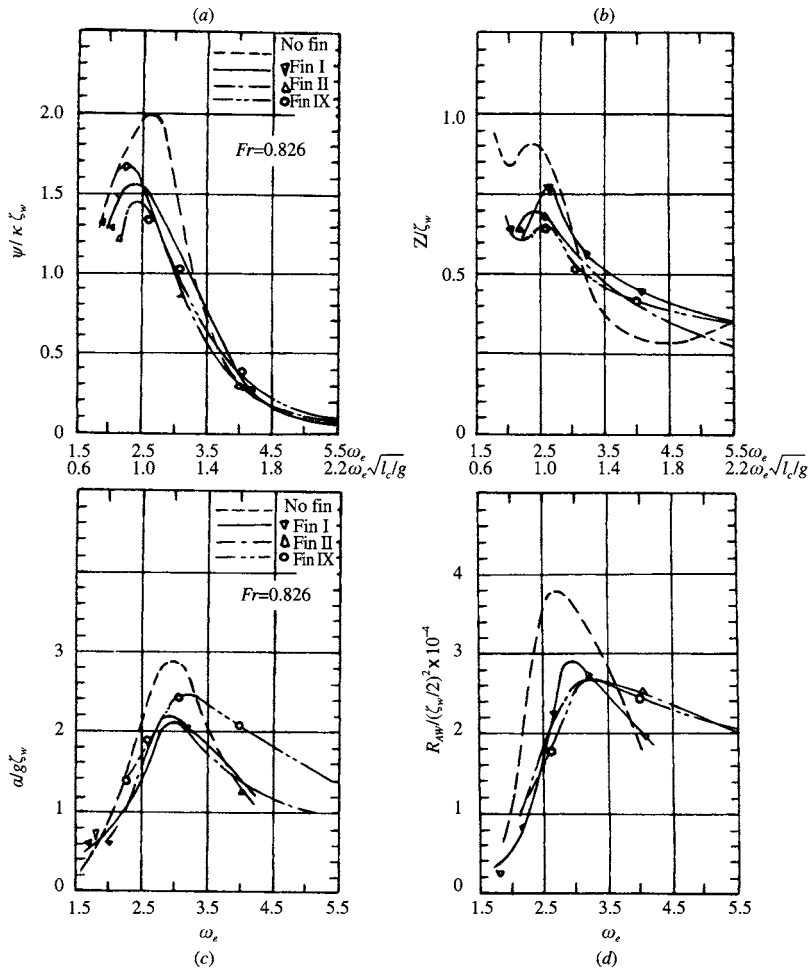


Fig. 8.36 Influence of bow hydrofoil of SES model on its seaworthiness. (a) Relative pitch angle versus relative encounter wave frequency; (b) relative heave amplitude versus relative encounter wave frequency; (c) relative vertical acceleration versus vertical acceleration at bow; (d) relative average drag increment of craft in waves.

Among them, on type I, i.e. the bow hydrofoil with side plates at an aspect ratio of 2 and an area ratio of 2% (namely the ratio of foil area to cushion area), mounted at inside of sidewalls, will be the better choice, which reduces the heave amplitude by 8–30%, pitch amplitude by 10–30%, vertical acceleration by 20–30% and wave drag by 15–45%. Meanwhile the bow hydrofoil was also mounted on SES test model 711-III in 1967 as shown in Fig. 1.32; the test proved that the bow hydrofoil could prevent plough-in and improve the seaworthiness of the craft.

Cushion flow rate

Increase the air flow rate into the bow/stern skirt and bag cushion pressure ratio so as to increase the pitch damping moment. The lift power will be increased following this measure.

Sidewall chines

The anti-spray plate on sidewalls for increasing pitch damping moment may also be a suitable measure for improving the seaworthiness of an SES. Figure 8.37 shows the test results of bow anti-spray plates on British SES HM.5. It can be found that bow acceleration can be reduced. With same reasoning, hard chine on sidewalls can also obtain the same results, just as the double hard chine on the sidewall lines of British SES HM.5.

Passive or active heave attenuation system and anti-roll systems

The fluctuation of cushion pressure of ACV/SES is unavoidable, as hovercraft run in waves; therefore some automatic control system for keeping cushion pressure constant will be the essential measure for improving the seaworthiness and reducing the vertical acceleration of ACV/SES. Some experiments for automatic discharge of cushion air have been carried out on the skirt test rig of MARIC and satisfactory results obtained. An automatic heave attenuation system was developed in the USA in the 1970s and produced the same results for reducing the cushion pressure fluctuation of an SES in waves follows:

1. automatic cushion air discharge apparatus to reduce the fluctuation of cushion pressure will be followed by an increase of fan air flow, otherwise the craft speed will drop down;
2. fan inlet/outlet valve regulation to adjust the cushion pressure;
3. automatic control of fan blades.

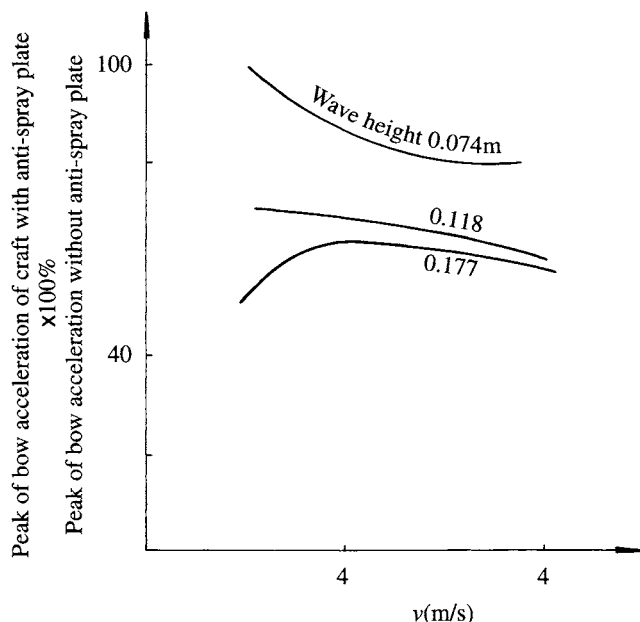


Fig. 8.37 Decrease of vertical acceleration of British SES due to the anti-spray plate on bow sidewall.

The latter two methods will save some lift power due to the lower flow rate consumption. Figure 8.38 shows the reduction of vertical acceleration in the navigation cabin of SES-200 by means of the ride control system (RCS). Thanks to the extreme reduction of pressure fluctuation, vertical acceleration was reduced significantly.

From Fig. 8.38 it can be seen that vertical acceleration was decreased to a satisfactory level, but accompanied by an increase of lift power of 15%. Figure 8.39 shows the improvement of seaworthiness of a high-speed test SES model SES-100A by means of an automatic control system. This equipment is also based on the theory of overpressure discharge and has the advantage of simple configuration, low cost and high efficiency. The figure shows that vertical acceleration can be decreased by ~50%.

Ability to maintain cushion-borne operation of ACV/SES in high waves

With respect to an ACV, since the aerodynamic momentum drag, aerodynamic profile drag and skirt drag comprise the most part of craft total drag, these drags will be significantly increased in the case of head-wind operation of craft. Under such conditions the craft will experience speed degradation not only due to the drag increase but also the light load of the air propellers, if they are fixed pitch propellers.

Thus the power output and thrust will be reduced with the same propeller revolutions. Combining the effect of both drag and thrust, the craft speed will be degraded even though under hump speed. Figure 8.40 shows this situation. Using controllable pitch air propellers, increasing the reserve power and improving the skirt design mentioned above are the most efficient correction measures.

The additional drag of craft in waves can be calculated. Because the wind speed is given, the aerodynamic profile and aerodynamic momentum drag can be calculated.

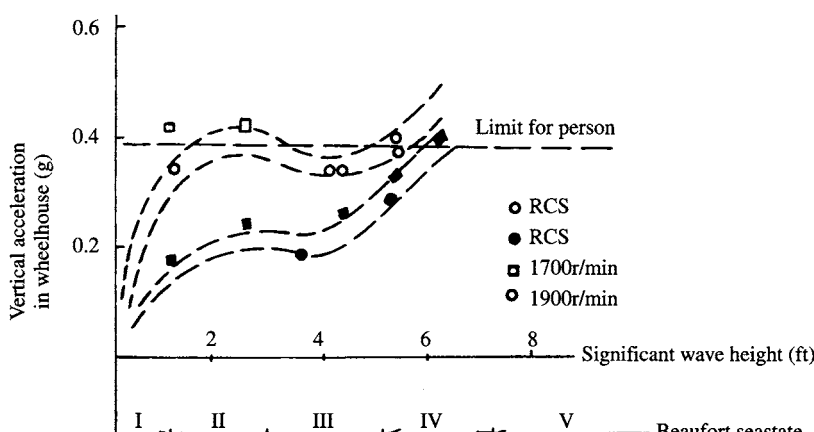


Fig. 8.38 Reduction of vertical acceleration in navigation cabin of SES-200 by operation of the ride control system (RCS).

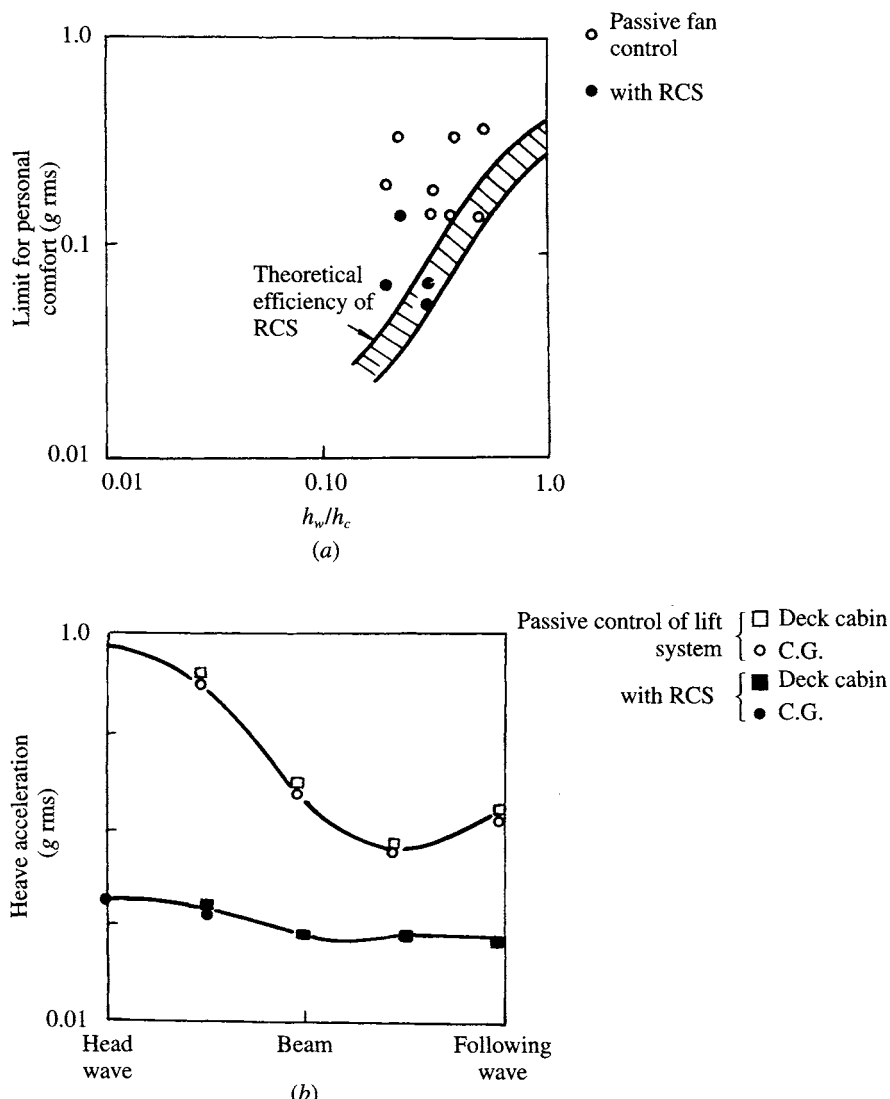


Fig. 8.39 Influence of RCS on seakeeping quality of SES-100A.

With respect to the wave drag, it can be calculated by the foregoing expressions. The additional drag of skirts in waves and can also be estimated by Fig. 8.41.

It is suggested that with respect to the ACV, particularly for small ACVs, the ability to maintain the cushion-borne operation of craft in waves has to be seriously considered, given that small wind and waves will affect the ability to maintain the cushion-borne operation, and the reserve power (or reserve thrust of the propellers) has to be considered in design.

From Fig. 8.40, it can be seen that it is impossible for the craft to take off in wind speed 5. Sometimes users ask for a lower designed calm water speed for some business

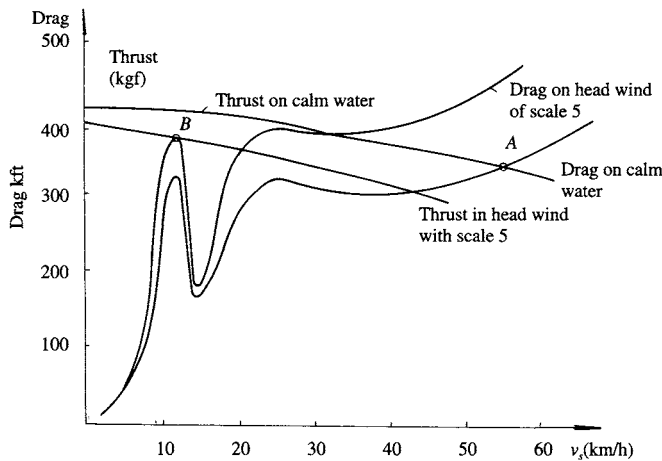


Fig. 8.40 Drag and thrust of an ACV in head seas.

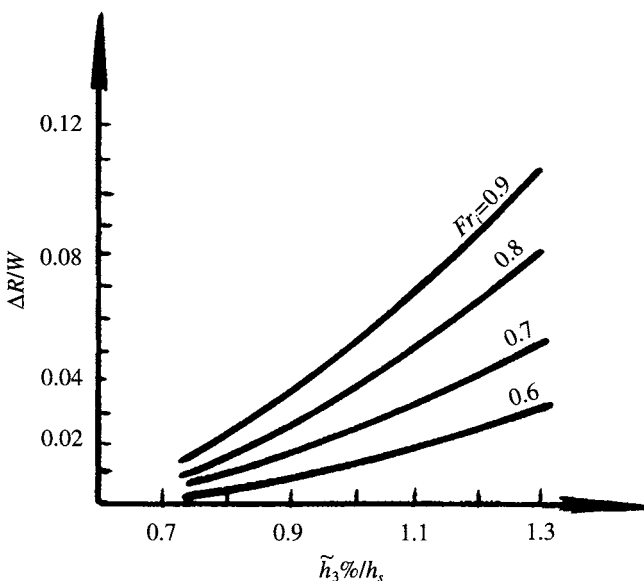


Fig. 8.41 The variation of relative additional drag of ACV in waves as a function of Froude Number and relative wave height.

consideration, but again demand the high weather limitation, namely the ability to maintain the cushion-borne operation in head wind. Then the two requirements contradict each other. The craft will have a given calm water speed to satisfy the user's requirements, but cannot maintain the cushion-borne operation under the given wind. Designers are most likely to have such experience with the design of small ACVs.

Effect of air flow rate and its distribution on seaworthiness

Effect of air flow rate

Air flow rate greatly affects the seaworthiness for both ACVs and SES, because the wave pumping, motion pumping, change of air leakage and compressibility of cushion air will affect the change of cushion pressure and flow rate. Figure 8.42 shows such dependency between the craft drag and air flow rate, but unfortunately we do not have concrete calculation methods to predict such a relation.

Perhaps such an influence can be obtained by means of a model test, when the principal dimensions of the craft, skirt configuration and lift system have been determined. Thus the influence of air flow rate on wave drag and also on the craft motion amplitude and acceleration can be estimated so as to determine the reserve power to meet the seaworthiness design requirement.

Effect of distribution of air flow rate

The distribution of air flow affects the seaworthiness of an SES, particularly on an SES running at high speed and in rough seas. The distribution of air flow on US SES-200B can be expressed as follows:

	Per cent of total		
Cushion pressure	4423	Pa	
Total flow rate	181.7	m^3/s	100.0
Flow rate blown directly into the cushion	113.0	m^3/s	62.0
Flow rate blown directly into the bow seal	22.6	m^3/s	12.5
Flow rate blown directly into the stern seal	45.0	m^3/s	25.5

These data were obtained by experiments.

With respect to craft at low speed, it is doubtful whether it is necessary. MARIC also has such experiments. Experiments of an SES model with two air ducts from the air outlet of the fan have been carried out in the towing tank. Part of the outflow may be led directly into the cushion and another part via air ducts, the bow/stern bag and through into the air cushion. The distribution of air flow can be regulated by a valve. The experiments did not obtain a clear conclusion. With such experiments with three parts of the air flow coming from the same source it might be difficult to get the expected results. But actually the air flow rate of bow/stern skirt on the Chinese SES-717 7203, 719, etc. are very small, sometimes even zero or a negative value.

Due to the lack of precise experiments and analysis as well as a suitable theoretical approach, it is difficult to estimate the influence of air flow distribution on seaworthiness. However, following the application of bow/stern responsive skirts to hovercraft, we are sure the air flow will have a definite effect on seaworthiness and maybe it is an important research theme for us in the near future.

Key observations

Seaworthiness of ACVs and SES plays a very important role in their performance. Assessment, particularly by analysis, is very complex and at present not completely developed and validated. If ACV and SES are to be developed further for operation

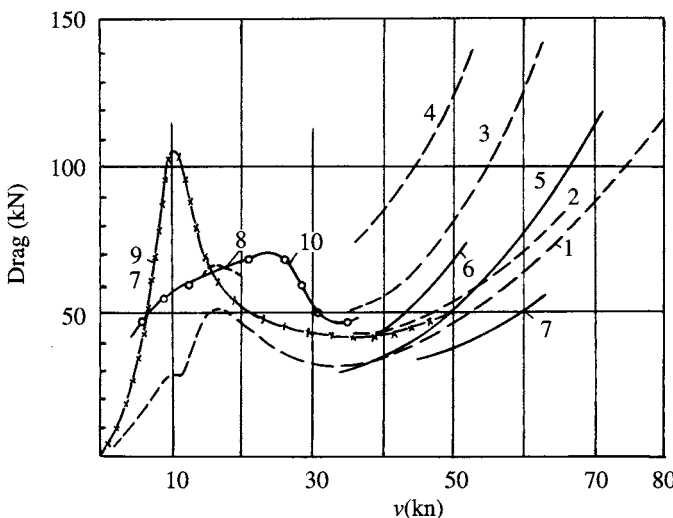


Fig. 8.42 Influence of air flow rate and wave height of SES weighing 80.7 t on craft drag: (1) on calm water; (2) in waves with height of $H_w = 0.33$; (3) $H_w = 0.5$; (4) $H_w = 0.7$; (5) $H_w = 1.4$; (6) $H_w = 0.3$, with the air flow rate $Q = 99-113 \text{ m}^3/\text{s}$; (7) $H_w = 0.6$, $Q = 99-113 \text{ m}^3/\text{s}$; (8) on calm water, $Q = 165 \text{ m}^3/\text{s}$; (9) the peak drag in waves with $H_w = 0.73\text{m}$; (10) passing through the peak drag for non acceleration operated mode of craft; (11) passing through the peak drag for accelerated operation of craft.

on open ocean seaways, further work to improve responsiveness is required. The following issues should be borne in mind by designers.

Pitch motions

Both ACVs and SES have small pitch damping and low pitch stability, therefore it is recommended to pay attention to resonance frequency for pitch motions. For example, according to calculation and experiments, the resonance relative pitch frequency of an SES weighing 100 t, $\omega_e(l_c/g)^{0.5} \approx 1.5-3.0$, i.e. $\omega_e \approx 3-6$. If the craft are running in waves with wavelength of 15–30 m at a speed of 35–40 km/h, then the craft are operating below resonance pitch frequency, hence craft are seldom over the critical condition when the craft are running in rough seas, and may develop significant response.

With respect to an ACV, although the craft can run at high speed, the inherent pitch frequency is also higher due to the larger pitch stiffness. Here, the resonant pitch relative frequency $\omega_e[l_c/g]^{0.5} \approx 5$. For an ACV weighing 70t at the speed of 40 knots, sometimes such an ACV also operates at critical or supercritical conditions, but due to the speed degradation of the ACV in waves, it also probably operates at subcritical conditions.

Thus it can be seen that increasing the pitch damping may be the critical measure for improving seaworthiness. Additional hydrofoils, anti-spray plates and bow side-wall configuration with a hard chine can solve such problems for an SES. Change of bag-cushion pressure ratio of the bow/stern skirt, the tightness of diaphragm of the D-type bag, area ratio of bag holes and various geometric parameters of responsive

skirts can also solve such problems for an ACV. Such parameters are best experimented with at model scale, or on full scale prototypes.

Heave motions

Both ACVs and SES possess large heave damping and heave stiffness, thus the amplitude peak will be located both on the high and low encounter frequency on the frequency response curve of heave (Figs 8.15(a) and 8.20), where the relative heave frequency $\omega_e [l_c/g]^{0.5} \approx 4\text{--}8$ (for SES) and 5 up to 15 (for ACV), which causes the high vertical acceleration associated with the cobblestoning effect which is also observed at high encounter frequency. For this reason, heave stiffness may need to be reduced by the following measures:

- using an automatic cushion pressure regulating control system, such as ride control systems (i.e. automatic air flow discharge system);
- using responsive skirt with low inherent frequency, i.e. positive control system, to improve the heave motion of craft;
- reducing the heave stiffness by means of using a rather flat fan characteristic curve and decreasing the air inlet/outlet pressure losses.

Speed degradation

Speed loss is always a troublesome problem faced by designers for both ACV and SES, because while the skirt components are in contact with the waves, they do not form a fine streamline, which induces significant wave drag. Figure 8.34 shows that speed degradation of ACV and SES is larger than deep submerged hydrofoil craft with automatic control systems and SWATH, therefore such problems are still an important research subject; perhaps the responsive skirt with large deformability will improve this problem.

Performance in head winds

Speed loss or even losing the above hump speed cushion-borne operation of an ACV running in head wind may be the most troublesome problem faced by designers and operators. This is due to the increase of drag and decrease of thrust; therefore designers have to pay serious attention to the problem to select engine, principal dimensions, to design propellers and skirt well as well as the lift system, etc. to keep the capability of cushion-borne operation of the ACV at given wind speed which is required by users.